ABSTRACT

The present Master's Thesis is part of the Master's degree in Nuclear Engineering of the *Universitat Politècnica de Catalunya* (UPC) and the *ENDESA Escuela de Energía*, and it was developed during the internship in the *Technische Universiteit Eindhoven* (TU/e).

The project shows the determination of the magnetic axis over time in the fusion reactor KSTAR.

During the project, different data is analysed, obtained from the diagnostic method Motional Stark Effect, and verified with *EFIT*. The data evaluation is done with the Interactive Data Language (IDL) code.

To start, an introduction to fusion is done by explaining some basic concepts, as what plasma is and how it is confined so energy will be generated, among other concepts. The characteristic parameters that define the KSTAR reactor are given as well.

Next, the physic principle of the MSE system is explained, as well as the instrumentation and its configuration and the data treatment.

Later, a brief explanation of the code development is done, trying to explain what was done for the data analysis and verification, and what possible further development can be done.

Finally, it is studied how the change of different parameters affects the magnetic axis over time in terms of the position, as the plasma current, the magnetic field or the plasma temperature. This is done by analysing different "shots".

The outcome of all is the demonstration of the MSE system as a reliable, strong and flexible tool for the control of the plasma equilibrium.

RESUMEN

El presente Trabajo de Final de Master forma parte del Master en Ingeniería Nuclear de la *Universitat Politècnica de Catalunya* (UPC) y ENDESA Escuela de Energía, y ha sido desarrollado durante el periodo de prácticas en la *Technische Universiteit Eindhoven* (TU/e).

El siguiente proyecto muestra la determinación del eje magnético y su evolución en el tiempo en el reactor de fusión KSTAR.

En dicho proyecto se analizan distintos datos, obtenidos mediante diagnóstico con *Motional Stark Effect* (MSE), y dichos datos se verifican con *EFIT*. Los datos son evaluados con el código *Interactive Data Language* (IDL).

Para empezar, se introduce el concepto de la fusión como técnica para crear energía, explicando algunos conceptos básicos cómo qué es el plasma y cómo confinarlo para poder así producir energía, entre otros. También se exponen los principales parámetros que caracterizan el reactor de fusión KSTAR.

Seguidamente, se explica el principio físico de funcionamiento de la técnica de medida MSE, así como la instrumentación y su configuración y el tratamiento de los datos.

A continuación, se explica brevemente el desarrollo del código, explicando lo que fue hecho para el análisis y la verificación de los datos, y se sugieren distintas posibilidades para un desarrollo futuro.

Finalmente, se estudia el efecto de distintos parámetros sobre la posición del eje magnético, como la intensidad de corriente, el campo magnético o la temperatura del plasma. Esto se lleva a cabo analizando distintos “disparos”.

De todo ello se concluye que el sistema MSE es una herramienta fiable, robusta y flexible para el control del equilibrio del plasma.

CONTENT

ABSTRACT i
RESUMEN ii
CONTENT iii
Figures v
Tables ix
Glossary xi
1. Preface 13
1.1. Project Origin 13
1.2. Motivation 13
2. Introduction 15
2.1. Objectives 15
2.2. Scope 15
2.3. Planning 16
3. Background 17
3.1. The current energy situation 17
3.2. Fusion and plasma 19
3.3. Plasma confinement 23
3.3.1. Plasma confinement: tokamak 24
3.4. Flux surfaces and q factor 27
3.5. KSTAR parameters 29
4. Motional Stark Effect 31
4.1. Justification 31
4.2. Physic principle 31
4.3. MSE system for KSTAR 33
4.3.1. Front end optical system 34
4.3.2. Filter 34
4.3.3. Detector 34
5. Code development 35
5.1. Determination of the magnetic axis 35
5.2. Verification of the results 37
5.3. Further development 38
6. Results 39

6.1. Plots 39
6.2. Comments on the results 63
CONCLUSIONS 65
APRECIATION 67
BIBLIOGRAPHY 69
Bibliographical references 69
Supplementary bibliography 69

Figures

Figure 3. 1: World electricity consumption prospects by region. 17
Figure 3. 2: World electricity generation evolution. [1]Excludes electricity generation from pumped storage. [2]Includes geothermal, solar, wind, heat, etc. [1] 18
Figure 3. 3: World electricity generation and related CO2 emissions. [2] 18
Figure 3. 4: Comparison of different types of power plants fuel consumptions to produce an electrical output of 1,000 MWe running for one year. [3] 19
Figure 3. 5: Average binding energy per nucleon. [4] 20
Figure 3. 6: Probability distributions of different fusion reactions. [3] 21
Figure 3. 7: Motion of a charged particle in different magnetic and electric fields configurations. 24
Figure 3. 8: Magnet system of a tokamak fusion device. [5] 25
Figure 3. 9: Schematic diagram of the components of a tokamak. [6] 26
Figure 3. 10: Flux surfaces for the MHD equilibrium model in polar toroidal coordinates. [7] 27
Figure 3. 11: Poloidal cross-section of the different flux surfaces topologies. (a) Flux surfaces in the unperturbed case, with the 2/1 resonant surface marked in blue. (b) Magnetic topology after the formation of a 2/1 magnetic island, with the island magnetic surfaces in red. [8] 29
Figure 3. 12: Toroidal view of the formation of an instability: the initially neatly nested magnetic surfaces (left) become deformed, giving rise to magnetic islands (right). [9] 29

Figure 4. 1: Representation of the Lorentz electric field direction from the result of a particle moving with a velocity v in a magnetic field B. [10] 31
Figure 4. 2: Stark Effect spectrum with the relation of the polarisation angle and the splitting lines angle. In blue the π lines and in red the σ lines. [10] 32
Figure 4. 3: Top view of the KSTAR tokamak with an indication of the 3 beams, the MSE lines of sight and the direction of plasma current and toroidal magnetic field. [10] 33

Figure 5. 1: Magnetic pitch angle over radius for t = 3 s for shot number 13693. 35
Figure 5. 2: Magnetic pitch angle and fitting parabolic function for over radius for t = 3 s for shot number 13693. 36
Figure 5. 3: Magnetic axis over time for shot number 13693. 37
Figure 5. 4: MSE magnetic axis compared with EFIT for shot number 13693 for the times 3.0 s, 3.01 s and 3.02 s. 38

Figure 6. 1: Plasma current (up) and NBI voltage (down), with ION1 blue, ION2 green, ION3 red, for shot 13691. 39
Figure 6. 2: Magnetic axis over time for shot 13691. 40
Figure 6. 3: Magnetic axis from MSE and EFIT, over t=2s – 3s for shot 13691. 40
Figure 6. 4: Plasma current (up) and NBI voltage (down), with ION1 blue, ION2 green, ION3 red, for shot 13692. 41
Figure 6. 5: Magnetic axis over time for shot 13692. 41
Figure 6. 6: Magnetic axis from MSE and EFIT, over t=2s – 3s for shot 13692. 42

Figure 6. 7: Plasma current (up) and NBI voltage (down), with ION1 blue, ION2 green, ION3 red, for shot 13693. 42
Figure 6. 8: Magnetic axis over time for shot 13693 43
Figure 6. 9: Magnetic axis from MSE and EFIT, over t=2s – 3s for shot 13693. 43
Figure 6. 10: Plasma current (up) and NBI voltage (down), with ION1 blue, ION2 green, ION3 red, for shot 13694. 44
Figure 6. 11: Magnetic axis over time for shot 13694 44
Figure 6. 12: Magnetic axis from MSE and EFIT, over t=2s – 3s for shot 13694. 45
Figure 6. 13: Plasma current (up) and NBI voltage (down), with ION1 blue, ION2 green, ION3 red, for shot 13724. 45
Figure 6. 14: Magnetic axis over time for shot 13724 46
Figure 6. 15: Magnetic axis from MSE and EFIT, over t=2.5s – 3.5s for shot 13724. 46
Figure 6. 16: Plasma current (up) and NBI voltage (down), with ION1 blue, ION2 green, ION3 red, for shot 13725. 47
Figure 6. 17: Magnetic axis over time for shot 13725. 47
Figure 6. 18 Magnetic axis from MSE and EFIT, over t=2.5s – 3.5s for shot 13725. 48
Figure 6. 19: Plasma current (up) and NBI voltage (down), with ION1 blue, ION2 green, ION3 red, for shot 13727. 48
Figure 6. 20: Magnetic axis over time for shot 13727. 49
Figure 6. 21: Magnetic axis from MSE and EFIT, over t=2.5s – 3.5s for shot 13727. 49
Figure 6. 22: Plasma current (up) and NBI voltage (down), with ION1 blue, ION2 green, ION3 red, for shot 13728. 50
Figure 6. 23: Magnetic axis over time for shot 13728 50
Figure 6. 24: Magnetic axis from MSE and EFIT, over t=2.5s – 3.5s for shot 13728. 51
Figure 6. 25: Plasma current (up) and NBI voltage (down), with ION1 blue, ION2 green, ION3 red, for shot 13903. 51
Figure 6. 26: Magnetic axis over time for shot 13903. 52
Figure 6. 27: Magnetic axis from MSE and EFIT, over t=3s – 4s for shot 13903. 52
Figure 6. 28: Plasma current (up) and NBI voltage (down), with ION1 blue, ION2 green, ION3 red, for shot 13904. 53
Figure 6. 29: Magnetic axis over time for shot 13904. 53
Figure 6. 30: : Magnetic axis from MSE and EFIT, over t=3s – 4s for shot 13904. 54
Figure 6. 31: Plasma current (up) and NBI voltage (down), with ION1 blue, ION2 green, ION3 red, for shot 13905. 54
Figure 6. 32: Magnetic axis over time for shot 13905. 55
Figure 6. 33: Magnetic axis from MSE and EFIT, over t=3s – 4s for shot 13905. 55
Figure 6. 34: Plasma current (up) and NBI voltage (down), with ION1 blue, ION2 green, ION3 red, for shot 13906. 56
Figure 6. 35: Magnetic axis over time for shot 13906. 56
Figure 6. 36: Magnetic axis from MSE and EFIT, over t=3s – 4s for shot 13906. 57
Figure 6. 37: Plasma current (up) and NBI voltage (down), with ION1 blue, ION2 green, ION3 red, for shot 14202. 57
Figure 6. 38: Magnetic axis over time for shot 14202. 58
Figure 6. 39: Magnetic axis from MSE and EFIT, over t=7s – 8s for shot 14202. 58
Figure 6. 40: Plasma current (up) and NBI voltage (down), with ION1 blue, ION2 green, ION3 red, for shot 14203. 59
Figure 6. 41: Magnetic axis over time for shot 14203. 59

Figure 6. 42: Magnetic axis from MSE and EFIT, over t=7s – 8s for shot 14203. 60
Figure 6. 43: Plasma current (up) and NBI voltage (down), with ION1 blue, ION2 green, ION3 red, for shot 14204. 60
Figure 6. 44: Magnetic axis over time for shot 14204. 61
Figure 6. 45: Magnetic axis from MSE and EFIT, over t=7s – 8s for shot 14204. 61
Figure 6. 46: Plasma current (up) and NBI voltage (down), with ION1 blue, ION2 green, ION3 red, for shot 14205. 62
Figure 6. 47: Magnetic axis over time for shot 14205. 62
Figure 6. 48: Magnetic axis from MSE and EFIT, over t=7s – 8s for shot 14205. 63

Tables

Table 3. 1: Characteristic parameters of the KSTAR reactor. (Source: NFRI) 30

Glossary

D (Deuterium): hydrogen stable isotope with one proton and one neutron. It is commonly represented as ^{2}H or D.

ECE (Electron Cyclotron Emission): optical diagnostic method by which the electron temperature is determined based on radio-frequency electromagnetic waves that electrons emit when gyrating around under the influence of a magnetic field.

EFIT: code that reconstructs magnetic equilibrium from the measurement of the magnetic pitch angle

(Nuclear) Fusion: nuclear reaction which two or more light nucleus collide and fuse and as a result a new heavier nucleus is created, releasing an important amount of energy. Fusion is the reaction that power the stars.

IDL (Interactive Data Language): programming language used for data analysis.

Isotope: nuclides of a chemical element with same proton number but different neutron number.

KSTAR (Korea Superconducting Tokamak Advanced Research): magnetic fusion reactor at the National Fusion Research Institute in Daejeon, South Korea. The reactor start-up on June 2008.

Magnetic axis: the axis of the unperturbed nested flux surfaces in a tokamak.

Magnetic pitch angle (γ_m): is the angle between the velocity vector of a charged particle and the local magnetic field in which the particle is moving.

MSE (Motional Stark Effect): active spectroscopy method by which the magnetic field in the plasma is determined based on the shifting and splitting of spectral lines due to Lorentz force when a neutral atom is moving in an electric field.

Plasma: "An ionized gas consisting of positive ions and free electrons in proportions resulting in more or less no overall electric charge, typically at low pressures (as in the upper atmosphere and in fluorescent lamps) or at very high temperatures (as in stars and nuclear fusion reactors)." (Oxford Dictionary, 2015)

Shot: every Neutral Beam Injection done to obtain data for the MSE analysis.

T (Tritium): radioactive isotope of hydrogen with one proton and two neutrons. It is commonly represented as ^{3}H or T.

Tokamak (***то**роидальная **ка**мера с **ма**гнитными **ка**тушками* – **to**roidal **cha**mber with **ma**gnetic **c**oils): torus shaped device based on the magnetic confinement to isolate the plasma from the walls.

Preface

1.1. Project Origin

The present Master's Thesis is part of the Master's degree in Nuclear Engineering of the *Universitat Politècnica de Catalunya* (UPC) and the *ENDESA Escuela de Energía*, and it was developed during the internship in the *Technische Universiteit Eindhoven* (TU/e).

The project shows the determination of the magnetic axis over time in the fusion reactor KSTAR.

During the project, different data is analysed, obtained from the diagnostic method Motional Stark Effect, and verified with *EFIT*. The data evaluation is done with the Interactive Data Language (IDL) code.

The code used for the data treatment is the Interactive Data Language (IDL), and different versions of the code are used depending on the working subdirectory.

The update of the code will allow the determination of the magnetic axis what will permit a control of the plasma equilibrium.

1.2. Motivation

After attending to the first year of the Master's degree in Nuclear Engineering, I decided to specialise in Fusion Technology and focus the end of master thesis on the analysis and treatment of data.

Nowadays, electricity is becoming the most used energy source in both the developed countries and the emergent countries, and some studios claim that it usage will exponentially increase by the years, so a reliable, safe and clean electricity production is needed, since the currently production path is not sustainable anymore.

As an electrical engineer my principal motivation is try to find a solution to the supplying energy problem, and I think fusion energy is the solution and the right way for it and for a sustainable world.

After taking the first year of the master, I realised about the enormous energy source the nuclear energy is. However, currently it is produced through fission, which has the main problem of radioactivity. On the other hand, with fusion the radioactivity issue is mostly reduced and it presents other advantages, as the production of more energy with less fuel and the use of water as fuel instead of uranium, a controversial material.

Other reason by which I decided to do this thesis is introducing me in the world of investigation on the fusion field, since it is a technology that needs further investigation and development, and to develop my skills in the usage of codes for the treatment and analysis of experimental data.

2. Introduction

2.1. Objectives

The principal objective of this thesis is to determine the magnetic axis of the plasma over time from the data measured with MSE system on KSTAR reactor, so the density current profile can be determined for a better control of the plasma stability. In order to be carried out, it is necessary to use the IDL code. In order to know if the results are trustworthy, the results are cross-checked with the results obtained with *EFIT*.

At the same time, a second objective is to learn to work with IDL code language for the data treatment as well as to achieve specific knowledge in analysing experimental data and be able to interpret the results and come to the proper conclusions.

2.2. Scope

As it is mentioned on the previous sections, the present project is focused on the determination of the magnetic axis over time with MSE system for the fusion reactor KSTAR. The tasks to be complete are structured on the next points:

- Study of the basic concepts related to fusion in order to have a background knowledge.
- Familiarization with the measurements systems, understanding the physic principles, the instrumentation used, what is measured and how the data is analysed.
- Creation of part of the code in IDL language to analyse the experimental data obtained with the MSE system and obtain the magnetic axis over time from the data.
- Verification of the results from MSE, understanding by verification that the results are as expected, by comparing them with the results from EFIT, assuming that the results from EFIT are right.
- Analysis of how different parameters affect to the position of the magnetic axis.

It is important to mention that it is out of the scope of this project the measurement of the experimental data. This data is provided and then processed and analysed. However, it is necessary to understand the physics beyond the measurement methods and how the instrumentation used for the data acquisition, for a better understanding of the results and in order to be able to interpret them.

2.3. Planning

With regard to the planning of the project, this is performed in 12 stages and on the approximate dates following the Gantt diagram, available the last version on the Annex A.

It is worthy to mention that the Gantt diagram is a useful and powerful tool for the organisation of a project. In this project, the original version has been modified while difficulties appear, mainly when it come about implementing the ideas on the code.

3. Background

3.1. The current energy situation

Present-day society use of energy has grown exponentially, as well as population, and it is expected to increase exponentially over the next years. The development of emerging countries, the automatization, the increasing use of electronic devices and the switching of traditional sources of energy in to electricity, among others, are demanding a stable and reliable energy supply.

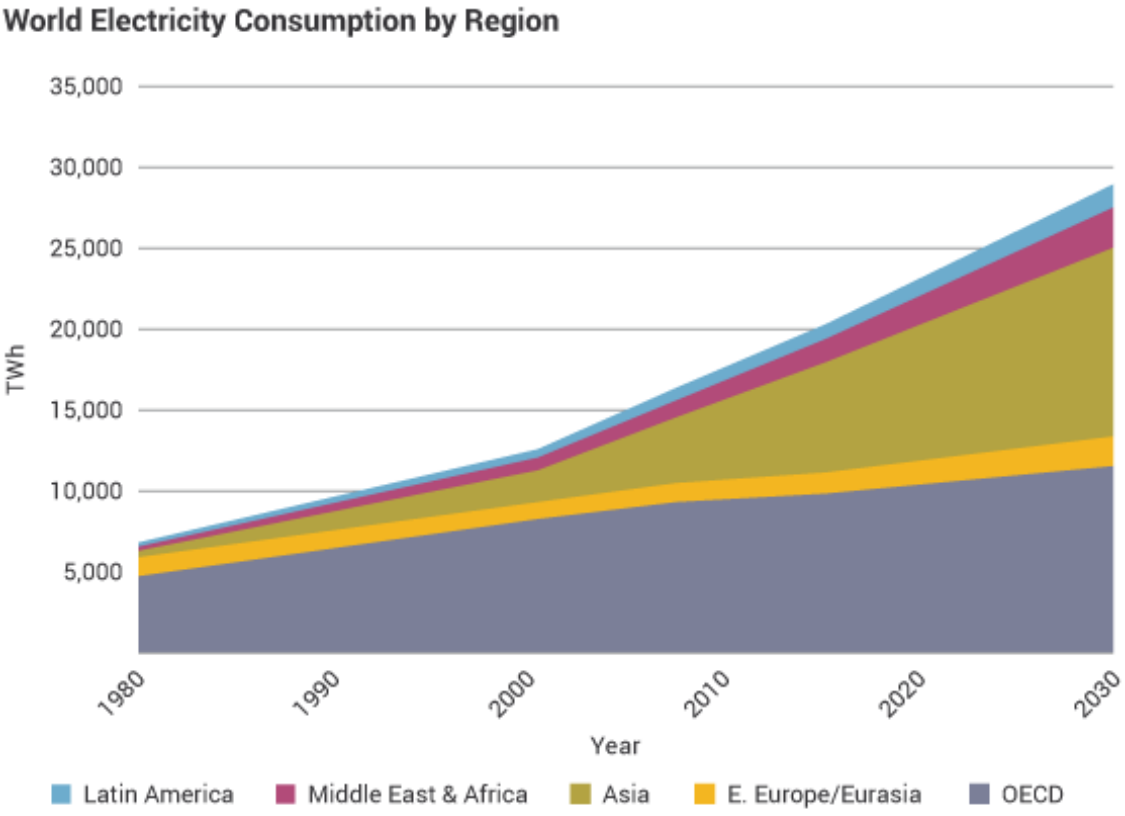

Figure 3. 1: World electricity consumption prospects by region.

Nowadays, the electricity production is mostly based on the fossil fuel, based on coal, gas and oil. This causes a great impact on the environment and in addition the energy industry cannot guarantee a large long-term supply since those resources are limited. Furthermore, the reserves come from unstable countries, resulting in the volatility on the price of the raw material and in geopolitical tensions in the areas of greatest reserves.

With regard to the renewable production, the industry cannot guarantee a regular grid supply due to the irregular production of some sources. Another important drawback is that they can only be developed in specific areas.

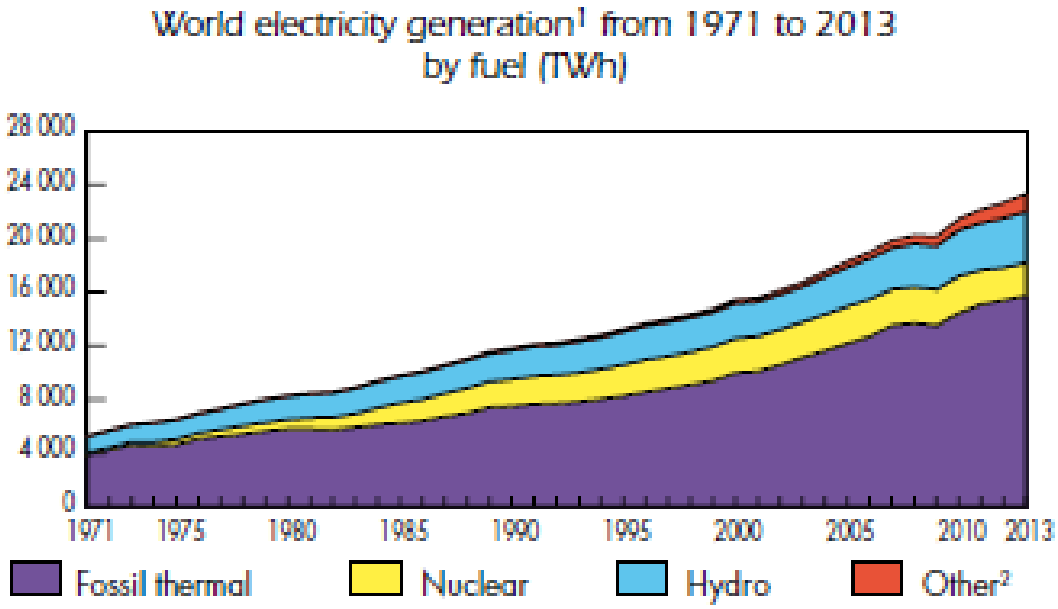

Figure 3. 2: World electricity generation evolution. [1]Excludes electricity generation from pumped storage. [2]Includes geothermal, solar, wind, heat, etc. [1]

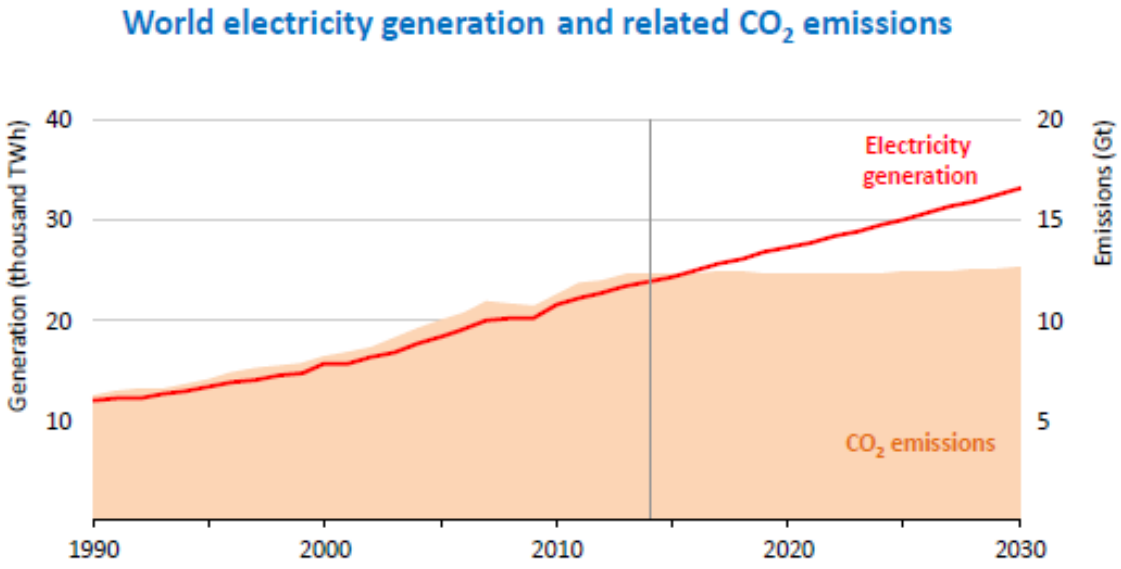

Figure 3. 3: World electricity generation and related CO2 emissions. [2]

The present situation has promoted the search for new viable energy sources and nuclear fusion is an excellent alternative to achieve an efficient large-scale supply. The main problem with this technology is the complexity of the field. There are many research paths and a big amount of global collaboration.

The principal advantages of fusion about the actual industries are:

- Zero emission of CO_2 or other pollutants when producing energy.
- No radioactive fusion products, with the exception of tritium which is treated inside the reactor using it as fuel.
- Use of water as fuel to power the fusion reactor, which is cheap and abundant.
- Use of very little fuel, and moreover logistical resources.
- Minimization of activated materials due to neutron contact, by using low activation materials with less than 100 years activation.

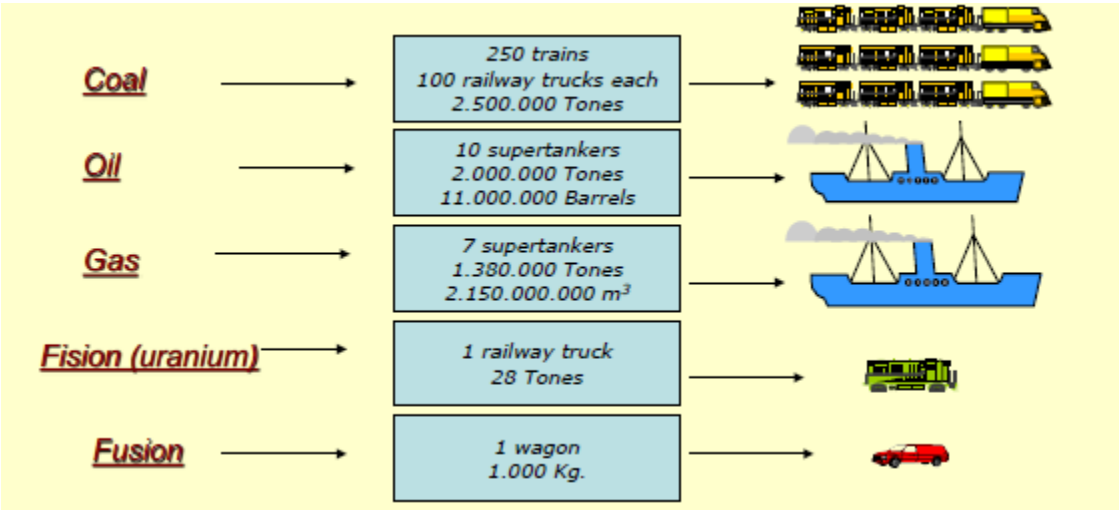

Figure 3. 4: Comparison of different types of power plants fuel consumptions to produce an electrical output of 1,000 MWe running for one year. [3]

3.2. Fusion and plasma

The fusion reaction is a nuclear reaction in which two or more nucleus collide and the result is another nucleus of a greater atomic weight. During the reaction, matter is not conserved since the total mass of the resulting nucleus is lower than the sum of the colliding nucleus, and the mass defect escapes as kinetic energy.

For fusion to take place, the nuclei must overcome the electrical repulsion between the protons in the nucleus (Coulomb interaction). This means that fusion reactions rather take place with light nucleus, since as lighter is the element, less protons it has, so less energy is required to counteract against the electric repealing force.

Figure 3. 5 shows the idea graphically, dividing the elements in two groups – fusion and fission – depending on the binding energy per nucleon. In other words, on the energy necessary to split the nucleus into its components.

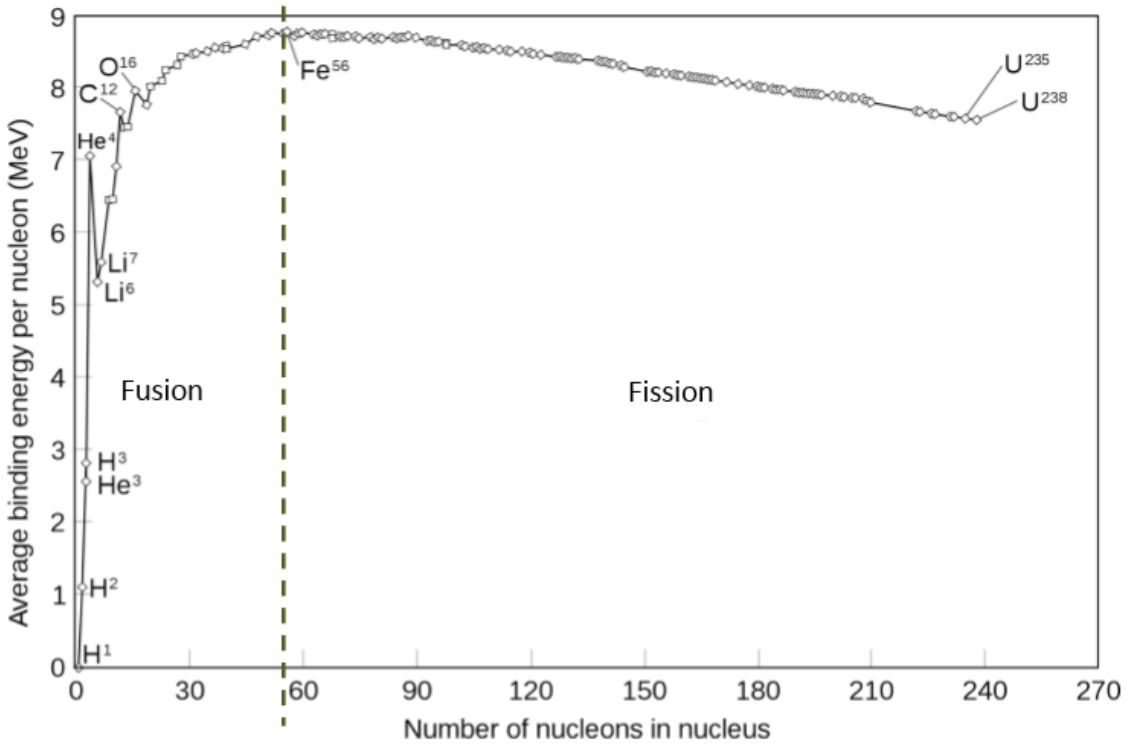

Figure 3. 5: Average binding energy per nucleon. [4]

The principal problem for fusion reactions to take place is that the nuclei will only collide with very high speed to weak the energy repulsion, which means that the temperature of the system must be considerably high (of the order of about 150 million degrees C). In other words, the probability that a reaction occurs depends on the temperature of the system. This is illustrated on Figure 3. 6.

Observing the Figure 3. 6 two important points are concluded: (1st) the reaction with highest cross section is the D-T reaction, hence it is the principal reaction that is wanted to take place at the reactor; and (2nd) the working temperature of the system for the reaction to occur is 10-20 keV. Fue to the high temperatures is fully ionized: it is in plasma state.

The D-T reaction is described as:

$$D + T \rightarrow He^4(3.5\ MeV) + n(14.1\ MeV) \tag{3.1}$$

Plasma is the fourth state of matter. It is characterised by the fact that it has positive and negative partciles instead of having the particles structured with a positively charged nucleus surrounded by electrons. The fuel in plasma state has to be confined in order to produce energy, and different systems exist based on inertial confinement or magnetic confinement. With regard to this project, the magnetic confinement is the system used.

In order to produce more energy than it consumes, the reactor has to work under the condition known as Lawson criterion, where n is the fuel density; T is the plasma temperature; and τ_E is the energy confinement time.

$$n\,\tau_E\,T > critical\ value \tag{3.2}$$

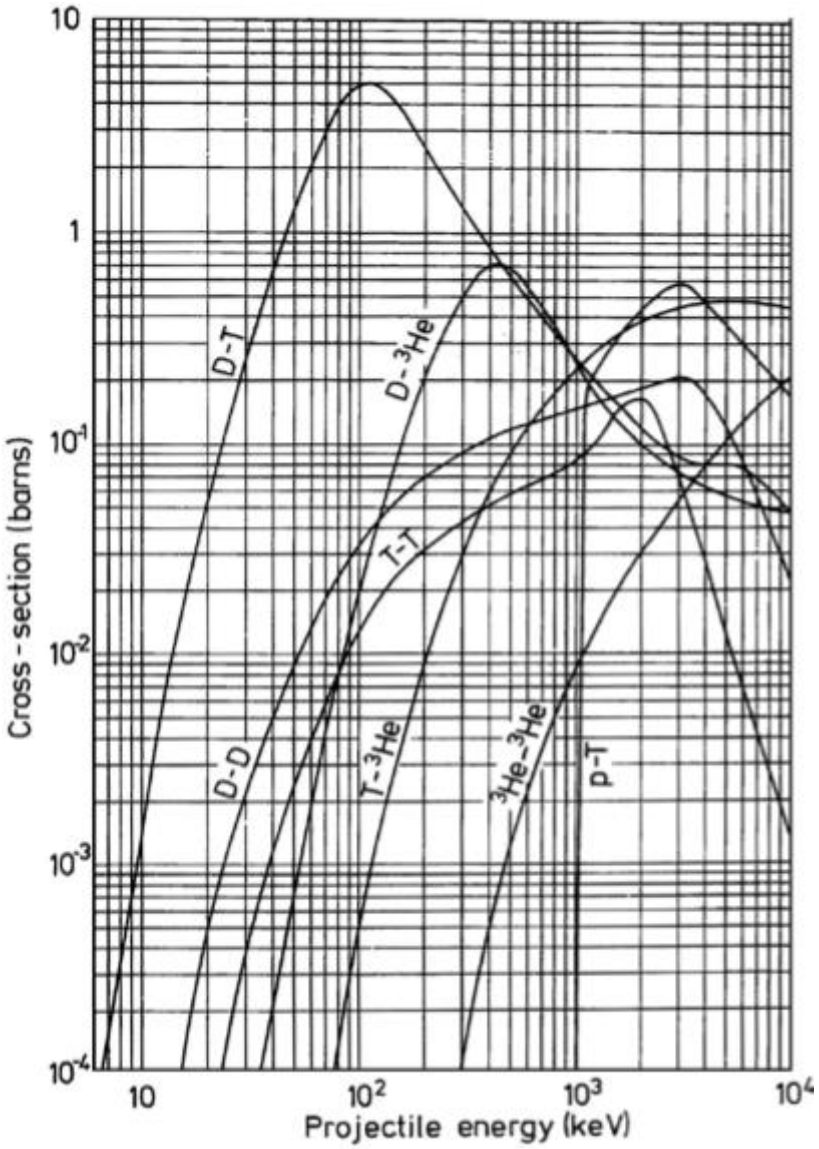

Figure 3. 6: Probability distributions of different fusion reactions. [3]

It is worthy to mention that not only D-T reaction takes place on the reactor, even though it is the one which will mostly occur and so the principal source of energy. Other important reactions that take place at a reactor are:

$$D + He^3 \rightarrow He^4(3.6\ MeV) + p(14.7\ MeV) \quad (3.3)$$

$$T + T \rightarrow He^4 + 2n + 11.3\ MeV \quad (3.4)$$

$$n_{Thermic} + Li^6 \rightarrow He^3 + T + 4.8\ MeV \quad (3.5)$$

3.3. Plasma confinement

As said on the previous point, the fuel for the fusion reactors is hydrogen fully ionized and the magnetic confinement, based on the application of a magnetic field, is the system used to confine the plasma in a specific volume.

The confinement of the plasma is necessary to counteract two phenomena:

- To balance the pressure gradient due to the difference in the plasma temperature between the centre and the edge, which pushes the plasma outward.

- To limit the mobility of the particles.

When applying a magnetic field to charged particles in motion, the particles gyrate. The fundamental motion of the charged particles in a magnetic field is described by the Lorentz force:

$$\overrightarrow{F}_{Lorentz} = q\,(\vec{E} + \vec{v} \times \vec{B}) \tag{3.6}$$

Where q is the charge of the particle; $\vec{E}$ is the electric field; $\vec{v}$ is the velocity of the particle; and $\vec{B}$ is the magnetic field. It has to be mentioned that due to the fact that plasma is formed by positive and negative particles, the Lorentz force pushes the two particles on different directions, creating charge separation and, furthermore, a voltage difference, so not only a magnetic field will affect the plasma particles, also an electric field will contribute to its motion.

However, charged particles follow different kind of movements and drifts depending on the configuration of the magnetic and electric field lines and gradients and the position between the fields. The principal effects in a tokamak can be summarised in:

a) In a homogeneous field, the particle will gyrate around a field line.

b) In a crossed electric and magnetic field, the particle will drift in the direction perpendicular to both fields.

c) In a gradient of a magnetic field, the particle will drift in the direction perpendicular to the gradient.

d) In a curved magnetic field, the particle will drift perpendicular to the plane in which the curved field line lies.

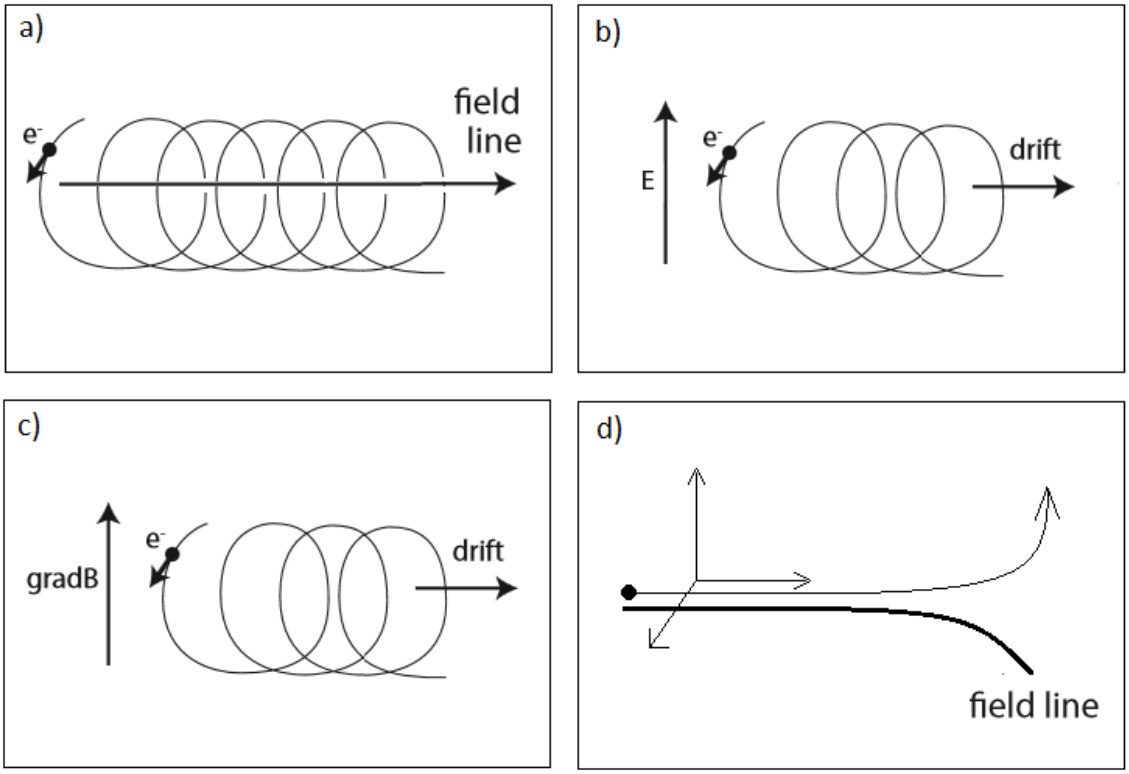

Figure 3. 7: Motion of a charged particle in different magnetic and electric fields configurations.

3.3.1. Plasma confinement: tokamak

The idea of the tokamaks is to achieve a stable plasma equilibrium and to keep the plasma in a volume using magnetic fields in different directions and of different strengths to take profit of the movements and drifts that charged particles experiment under its effect, isolating the plasma from the walls of the structure.

The tokamak is a closed system with toroidal configuration, in which the field lines are twisted in order to avoid different instabilities caused by the closing of the field lines over their selves. This is achieved by the combination of different magnetic fields and a resulting field is in a helical shape.

- Toroidal field: the magnetic field in the toroidal direction is generated with external coils around the torus. This field is constant in time and the strongest one. The primary function is the reduction of heat loss.

- Poloidal field: the poloidal field is generated by running a toroidal current in the plasma, generated inductively by using the plasma ring as the secondary winding of a transformer. The principal drawback is that this field is not constant in time. Compared to the toroidal field is an order of magnitude smaller. The principal functions are to balance the pressure and to introduce the rotational transform to avoid the charge separation.

- Vertical field: the field in the vertical direction is generated with coils above and under the plasma. The field is an order of magnitude smaller than the poloidal field. The main function is to balance the 'hoop force' resulting from the pressure in the plasma ring, which has the tendency to increase its radius.

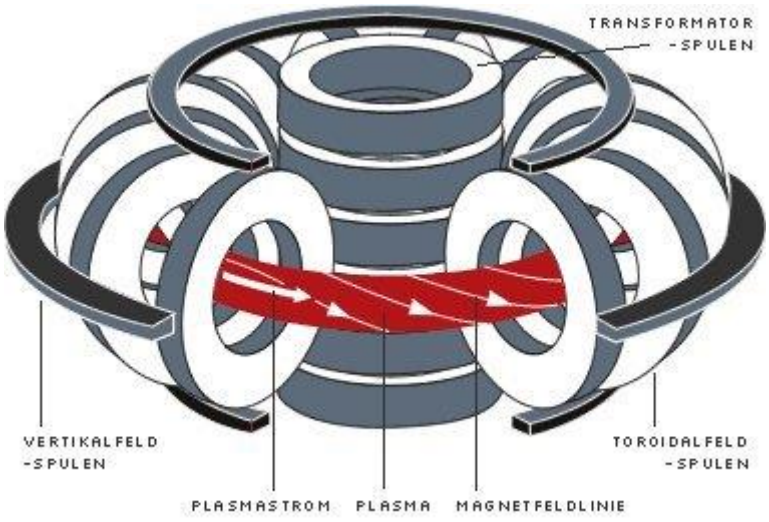

Figure 3. 8: Magnet system of a tokamak fusion device. [5]

A part from this three principal magnetic fields, also other coils are place around the tours of the tokamak to shape the plasma and control the vertical position.

The main components that conform a tokamak are:

- The magnets. Different magnets are placed in the structure to create the helical magnetic field that will confine, control and shape the plasma. The magnets that conform the system are the toroidal coils, the poloidal coils, the correction coils and the central solenoid.

- The vacuum vessel, inside which the plasma is confined and the fusion reactions take place. It is the first safety barrier against radioactivity.

- The blanket, that covers the inner walls of the vacuum vessel, extracts the heat by slowing down the neutrons. Hence it also protects the structure from the high-energy neutrons.

- The divertor. It is placed at the bottom of the vacuum vessel and it supports a very high heat flux. It also minimizes the contamination at the plasma by extracting ashes produced during the fusion reactor.

- The cryostat chamber surrounds the vacuum vessel and magnets to ensure a cool environment.

But other components and systems are needed to run the tokamak. This are the supporting systems:

- Tritium breeding;
- Cooling water;
- Diagnostic instrumentation;
- Remote handling;
- Heating and current drive;
- Vacuum system;
- Power supply;
- Fuel cycle system.

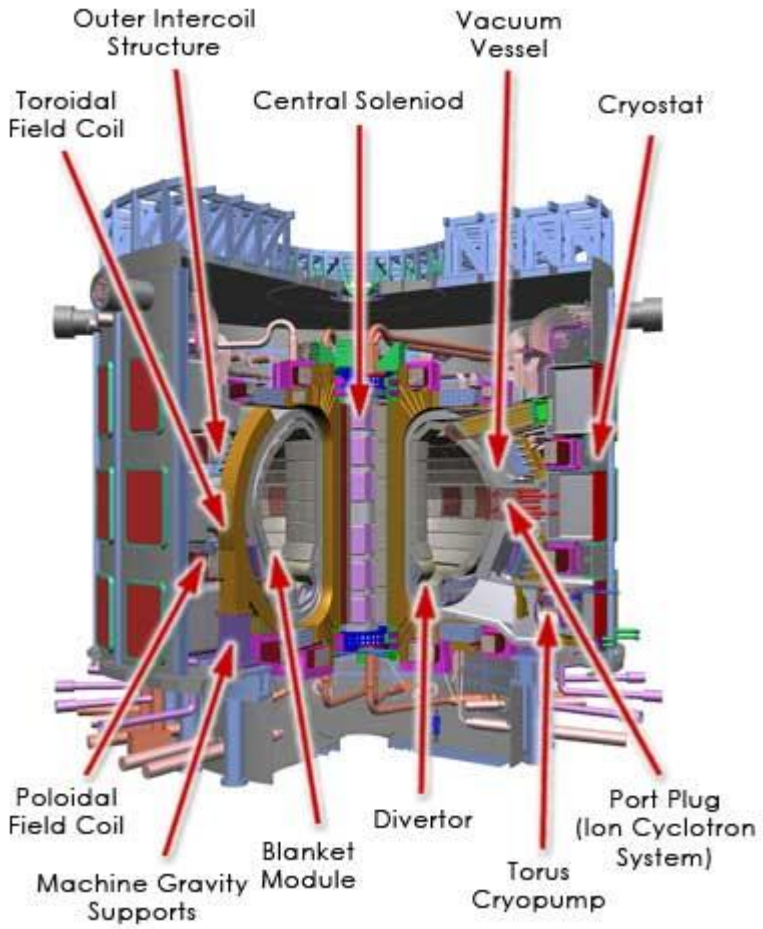

Figure 3. 9: Schematic diagram of the components of a tokamak. [6]

It must be highlighted that the operation of this types of reactors is pulsed. The inductive current drive is based on a time derivative of the magnetic flux, and this flux cannot grow indefinitely so at some point the transformer will saturate. The transformers work in AC, so they work with a positive half wave and a negative. If the reactor would work with both of them, the plasma would turn direction every time the half wave would change the sign. For this reason, these reactors must work with wave pulses with the same sign. Although, the half-period can be shaped so the plasma current can by driven for some minutes.

3.4. Flux surfaces and q factor

The objective of the magnetic system in a tokamak is to create a magnetic field which lines lie on nested toroidal surfaces: each surface has its own helical magnetic field. They are called flux surfaces.

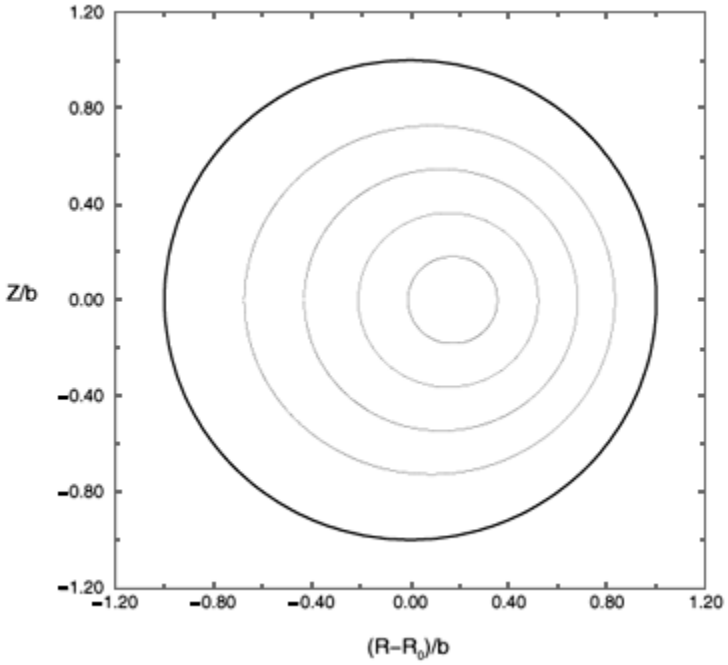

Figure 3. 10: Flux surfaces for the MHD equilibrium model in polar toroidal coordinates. [7]

An important characteristic of this surfaces is that in each of them different parameters are constant, such as temperature, pressure, poloidal magnetic field and current density. Moreover, all the surfaces have a single magnetic axis, corresponding the magnetic axis with the inmost flux surface, which is only a line.

Another important parameter that is also characteristic of each flux surface is the safety factor q defined as the number of toroidal turns a field line makes to complete one poloidal turn. Considering the torus as a cylinder, the q factor depending on radius of the flux surface r is described by:

$$q(r) = \frac{r\,B_T}{R\,B_P} \tag{3.7}$$

where B_T is the toroidal magnetic field strength; R the major radius of the cylinder (of the tours); and B_P the poloidal magnetic field strength. The toroidal field is externally applied and its different values for each flux surface is already known.

On the other hand, the poloidal field generated by the plasma current is:

$$B_P = \frac{\mu_0 I(r)}{2\pi r} \tag{3.8}$$

where $\mu_0 = 4\pi \cdot 10^{-7}\ T \cdot m/A$ is the vacuum permeability constant; and $I(r)$ the toroidal current depending on r.

$$I(r) = 2\pi \int j(r)\, r\, dr \tag{3.9}$$

where $j(r)$ is the current density. The problem is that the known parameter is the total current, but not the current in each flux surface. Hence, there are only two radii at which the q profile can be clearly determined: (1) at the magnetic axis; and (2) at the edge of the plasma. Between this two points, $q(r)$ is determined by the integral of $j(r)$.

Therefore, it is necessary to determine the magnetic axis, which it may be different to the geometrical centre of the tours – shift known as Shafranov shift, to optimize the confinement and stability of the plasma by shaping the q factor. The magnetic axis is placed where the magnetic poloidal field B_P is equal to zero.

At the magnetic axis the q factor is fully determined by the current density $j(0)$. For a circular plasma it is:

$$q(0)_{cyl} = \frac{1}{R\, d[\tan(\gamma_p)]/dr|_{r=0}} \tag{3.10}$$

where $\gamma_p = \tan^{-1}[B_P(r)/B_T(r)]$ is the pitch angle of the magnetic field. The q factor is related to the pitch angle by:

$$q(r) = \frac{r}{R \tan[\gamma_p(r)]} \tag{3.11}$$

With regard to the q factor value at the edge of the plasma, it is determined by the total plasma current I_P.

It is worthy to mention that the flux surfaces degenerate and become a volume, phenomenon known as magnetic island. This may happen when a field line pick up a perturbation from a perturbing field with a spectrum of spatial frequency resonant with the field line, displacing in radial direction the field line. Each island has a magnetic axis, wound around the original magnetic axis.

The magnetic islands are a topological property of the field. The problem comes when islands overlap. At this point, the field becomes chaotic, in which case the confinement can be seriously deteriorated.

Another important consequence of the magnetic islands are the disruptions. If magnetic islands are formed at the flux surface where $q = 2$ (close to the wall), they become very large leading to a chaotic field. In this case, the heat conduction from the centre to the wall will be strongly intensified, and the plasma will cooldown in a fraction of a millisecond. The consequences are catastrophic for the all device. Melting of the components facing the plasma or damaging or the metallic structure by the electrons that scape accelerated from the disruption are an example of the consequences.

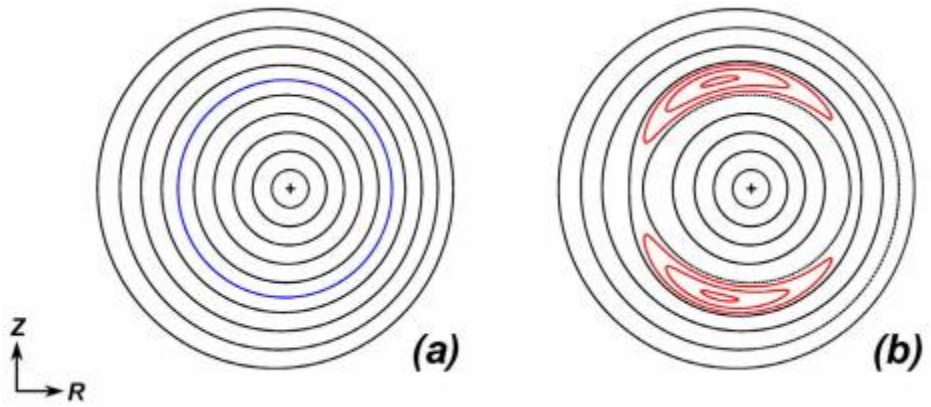

Figure 3. 11: Poloidal cross-section of the different flux surfaces topologies. (a) Flux surfaces in the unperturbed case, with the 2/1 resonant surface marked in blue. (b) Magnetic topology after the formation of a 2/1 magnetic island, with the island magnetic surfaces in red. [8]

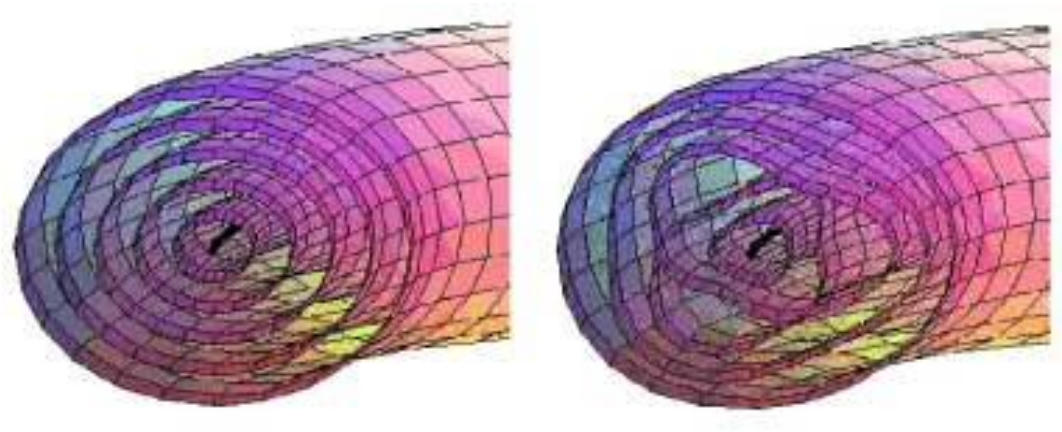

Figure 3. 12: Toroidal view of the formation of an instability: the initially neatly nested magnetic surfaces (left) become deformed, giving rise to magnetic islands (right). [9]

3.5. KSTAR parameters

There are different parameters that define a tokamak device and limit the achievable plasma geometry. This are the geometrical parameters in a tokamak, which determine the size of the vacuum vessel. But there are also other parameters that define a tokamak, related to the engineering field.

The parameters that define the KSTAR reactor are presented in the Table 3.1

	PARAMETER	VALUE
Geometrical	Major radius R_0	1.8 m
	Minor radius a	0.5 m
	Elongation k	2.0
	Triangularity δ	0.8
	Plasma volume	17.8 m^3
	Plasma surface area	56 m^2
	Plasma cross section	1.6 m^2
	Plasma shape	DN, SN
Engineering	Plasma current I_P	> 2.0 MA
	Toroidal field B_0	> 3.5 T
	Pulse length	> 300 s
	β_N	~ 5.0
Design – technology	Plasma fuel	H, D-D
	Superconductor	Nb_3Sn, NbTi
	Auxiliary heating /CD	~ 28 MW
	Cryogenic	9 kW at 4.5K

Table 3. 1: Characteristic parameters of the KSTAR reactor. (Source: NFRI)

4. Motional Stark Effect

4.1. Justification

The Motional Stark Effect (MSE) is a technique based on the analysis of the light produced by a neutral beam. With it, one can determine the pitch angle of the magnetic field so the current density profile can be calculated. This along with the diagnosis of the temperature, the particles density and the external magnetic field are used to achieve the plasma equilibrium.

By measuring the magnetic pitch angle, the radial q profile can be determined (Equation 3.11) and furthermore the density current profile. The q profile can be shaped as desired in order to optimize the confinement and stability of the plasma by adjusting the value of different parameters in the tokamak, such as the total plasma current or the toroidal magnetic field.

But for the determination of the q profile it is necessary to know the position of the magnetic axis. The magnetic axis of the flux surfaces is placed at the point where the poloidal magnetic field is zero, so the pitch angle is zero as well.

4.2. Physic principle

The MSE diagnosis measures the light emitted from an H neutral beam, which is inserted in the plasma. The beam is excited via collisions with the plasma, and then emits visible light. The beam atoms experiment an electric field since they are moving with a certain velocity v in a magnetic field B (Lorentz electric field, equation 4.1) which makes the light to split in nine spectral lines: three central σ lines and six outer π lines. This is known as Stark Effect.

$$E_{Lorentz} = v \times B \tag{4.1}$$

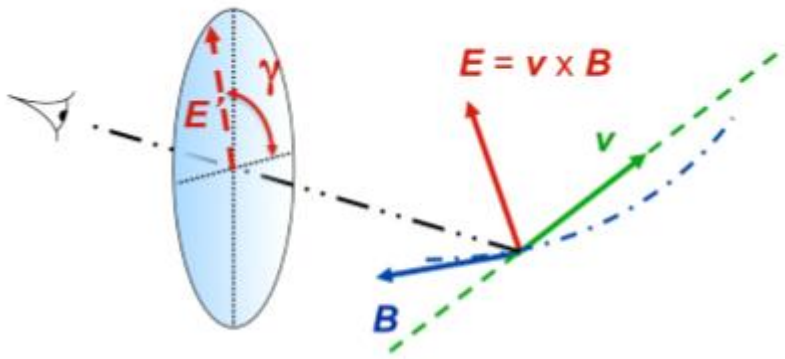

Figure 4. 1: Representation of the Lorentz electric field direction from the result of a particle moving with a velocity v in a magnetic field B. [10]

The electric field $E_{Lorentz}$ direction will be in the same direction as the magnetic pitch angle, since the polarization angle γ is directly proportional to the magnetic pitch angle γ_p. The polarization angle can be obtained from the Stark spectrum, along with other information:

- The size of the wavelength depends on:

$$\lambda = |v \times B| \tag{3.2}$$

- The intensity ratio of σ and π lines depends on the angle between the line of sight and $v \times B$.

- π lines angle is the same as the polarization angle γ. They are parallel with the electric field $E_{Lorentz}$.

- σ lines angle is $\pi/2$ step forward respect the polarization angle γ. They are perpendicular respect the electric field $E_{Lorentz}$.

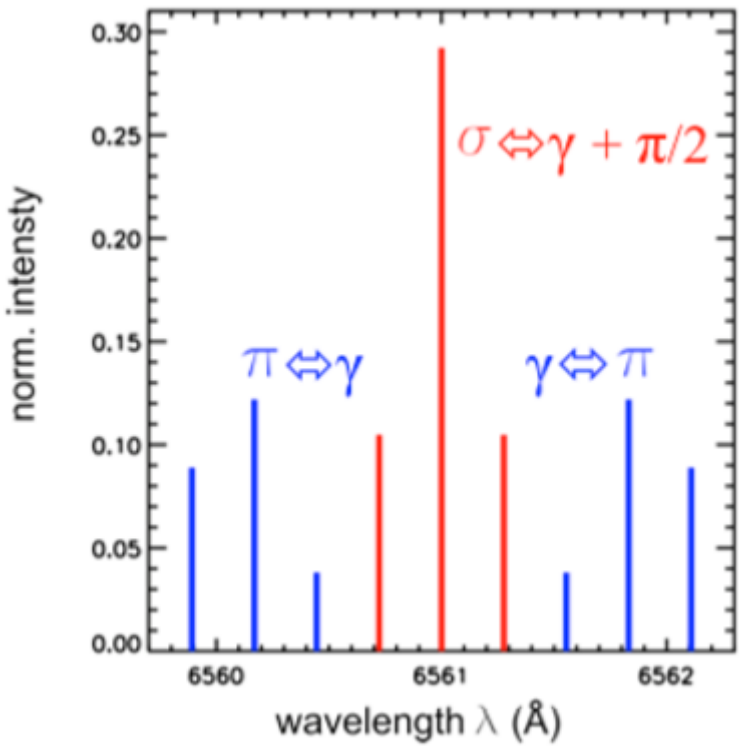

Figure 4. 2: Stark Effect spectrum with the relation of the polarisation angle and the splitting lines angle. In blue the π lines and in red the σ lines. [10]

The idea of the MSE system is that by measuring the intensity of light of the split lines, the polarization angle is calculated.

4.3. MSE system for KSTAR

On this section a brief summary of the document “A conventional Motional Stark Effect diagnostic for KSTAR” [10] is done, highlighting the most important aspect of the MSE system at KSTAR. For specific information, address to the original document.

The MSE system in the KSTAR has horizontal lines of sight. The Neutral Beam Injection consist of three ion sources ION1, ION2 and ION3 that will provide three different beams.

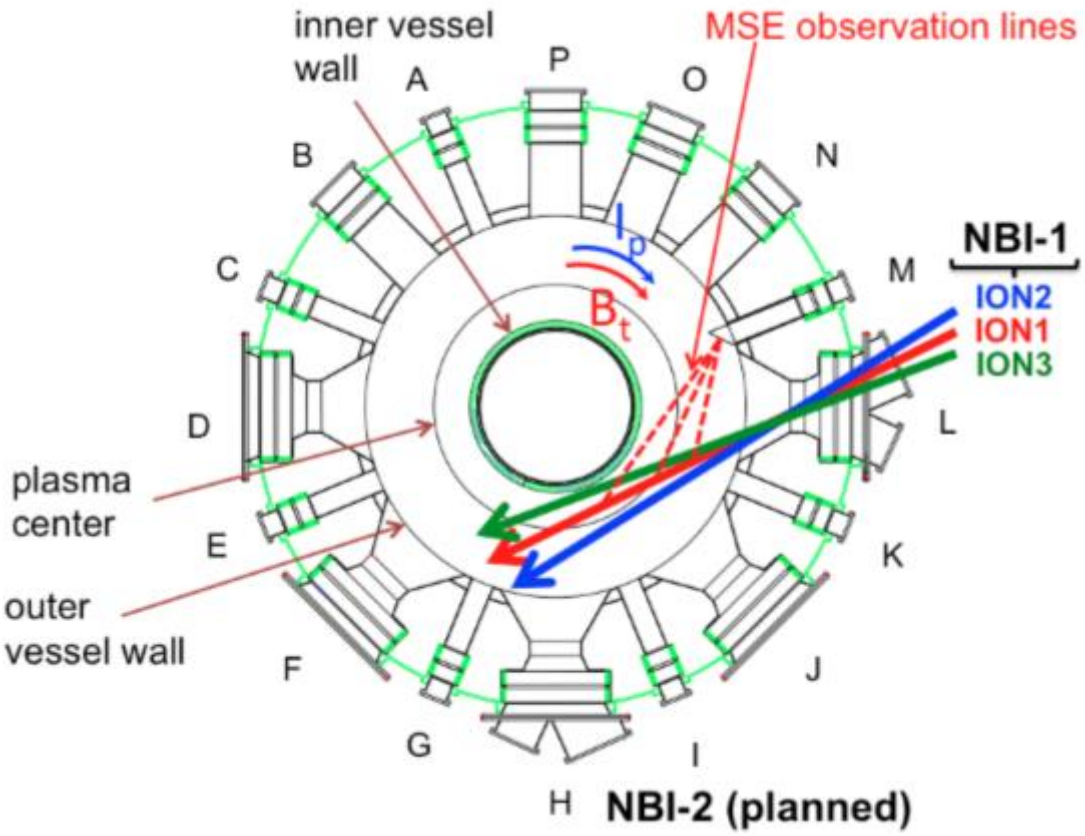

Figure 4. 3: Top view of the KSTAR tokamak with an indication of the 3 beams, the MSE lines of sight and the direction of plasma current and toroidal magnetic field. [10]

The number of channels to be used for the MSE system is determined by the absolute minimum spatial resolution of the point-spread-function of the emission profiles of the different ion sources. It is concluded that 25 inner channels cover the range $R = 1.74\,m - 2.22\,m$ with a spacing of 0.02m; and 5 more outer channels cover the range $R = 2.24\,m - 2.28\,m$ with 0.01m spacing.

The measuring system is divided in three sections: (1) Front end optical system; (2) filter; and (3) detector.

4.3.1. Front end optical system

This system is formed by different components, that due to the fact of the specific requirements of the system, need to be in a certain order, which is as follow: PEMs, collection lens, mirror, dichroic beam splitter, polarizer, optical fibres.

4.3.2. Filter

The main issue to select the filter is the wavelength. To avoid possible overlaps on the data measured from MSE, it has to be selected a filter with a wavelength with the minimum value of the red shifted π peaks. In the KSTAR this is around the 660 nm.

It is concluded that the filters have to be two cavity interference type with $\Delta\lambda_{FWHM,0} = 0.3\ nm$

4.3.3. Detector

In the end, what is going to be detected is photons. Due to the transmission losses through all the components that conform the MSE data acquisition system, the estimated collected photons at the detector is $6.5 \cdot 10^8\ photons/s$.

Based on the Signal to Noise Ratio as a function of photon rate detected, an avalanche photodiode detector (APD) is selected as the best option. This kind of detectors need DC bias voltage supply and require an amplification circuit to convert the current detecting signal into voltage. It is decided to use an off-the-shelf APD module.

5. Code development

With the developed code during this project, the aim to achieve is to obtain the magnetic axis from the polarization angle obtained with the MSE analysis, using the IDL language.

The code development is divided in two main stages:

1. Determination of the magnetic axis.
2. Verification of the results

When analysing the data with MSE, different parameters to run the code have to be set, such as the shot number, the beginning and ending time of the shot.

5.1. Determination of the magnetic axis

The input for the determination of the magnetic axis is the magnetic pitch angle over a determined radius fixed by the position of the detecting channels. This magnetic pitch angle is for a single time, as observed on the Figure 5.1

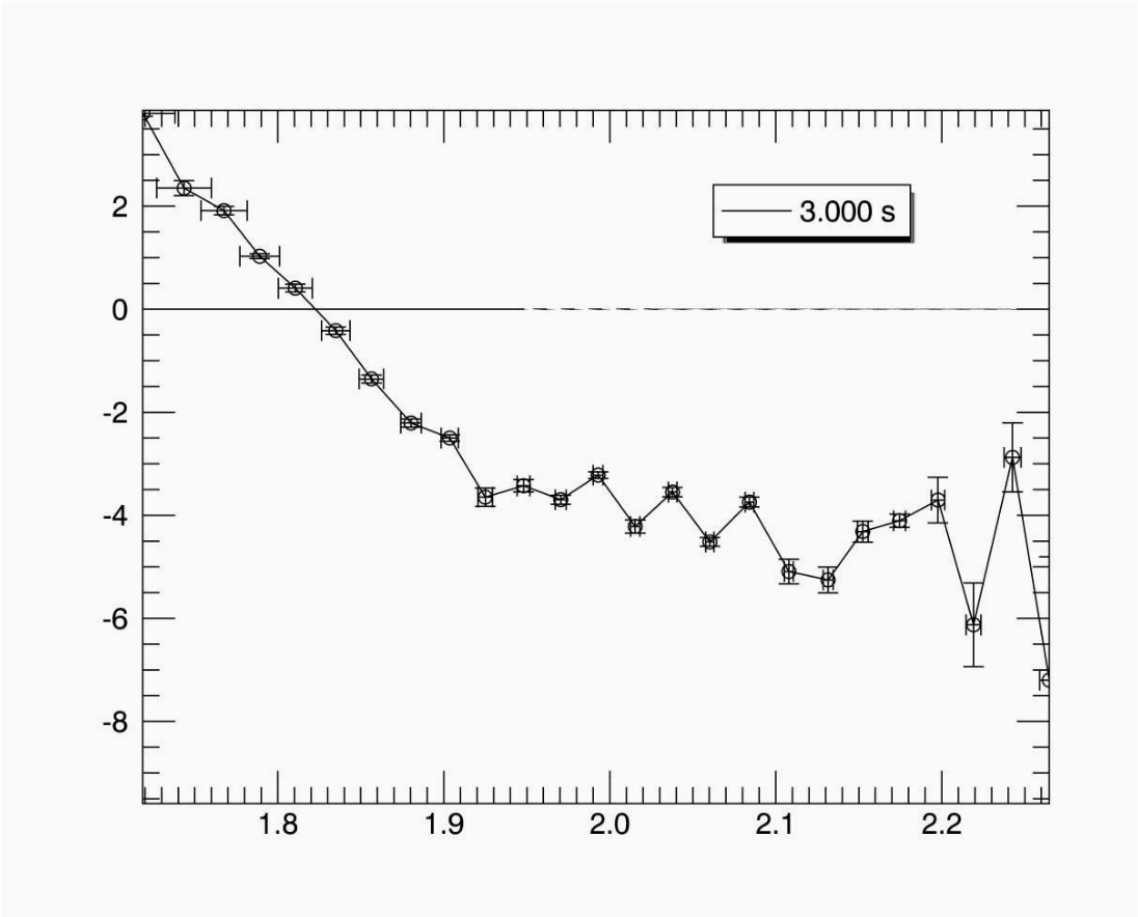

Figure 5. 1: Magnetic pitch angle over radius for t = 3 s for shot number 13693.

The next step is to write a new part on the code that fits the data in a parabolic function for a single time, taking into account that some channels have to be excluded since they deviate from the interesting region. Once the fitting curve is done, it has to be determined the point at which the magnetic pitch angle is equal to zero. This is done by interpolation.

This two processes might have and introduce and error to result, but when it is tried to compute this error, the result is that the error is too big (more than 5 cm), hence it is decided that for the moment no error bars are introduced neither in the fitting function nor in the interpolation.

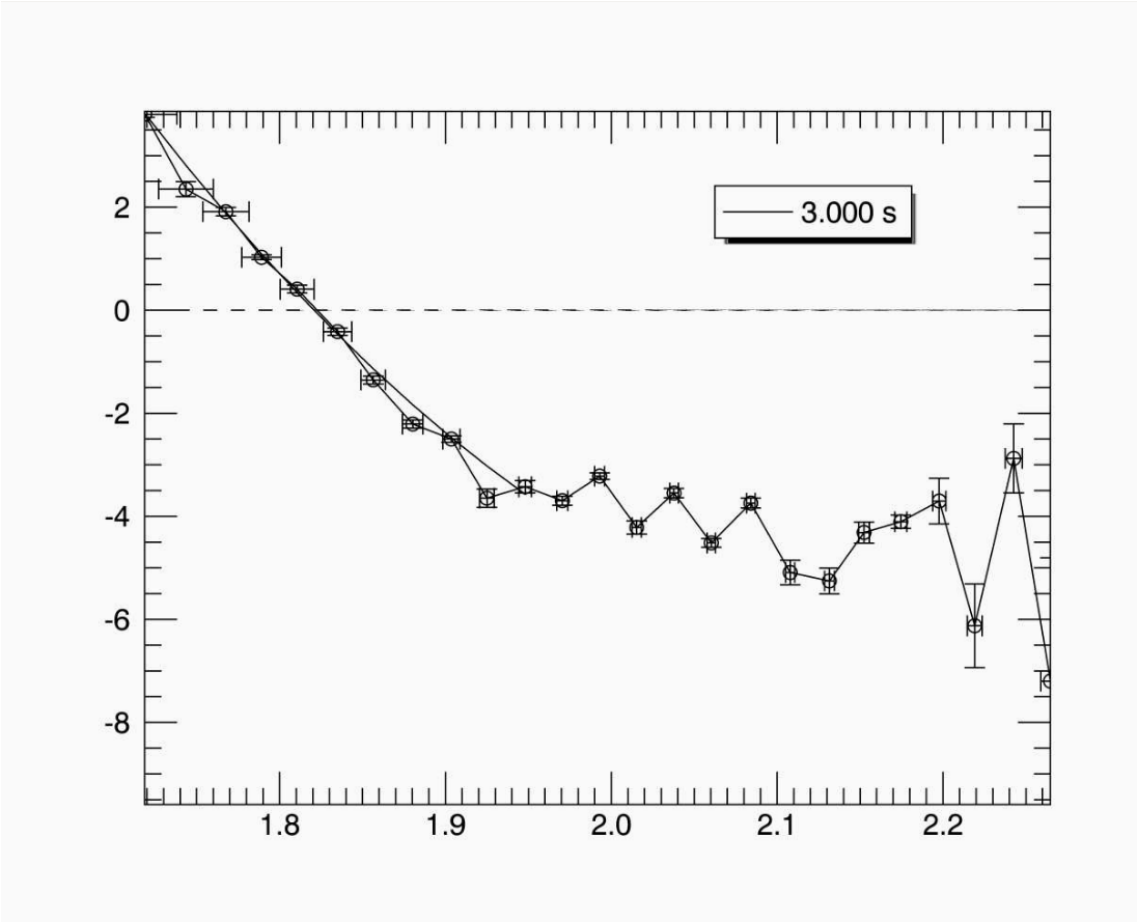

Figure 5. 2: Magnetic pitch angle and fitting parabolic function for over radius for t = 3 s for shot number 13693.

Later on, to obtain the magnetic axis over time, a loop is created that goes through all the times and channels, storing the data in a string that later on will be the data to plot the magnetic axis over time.

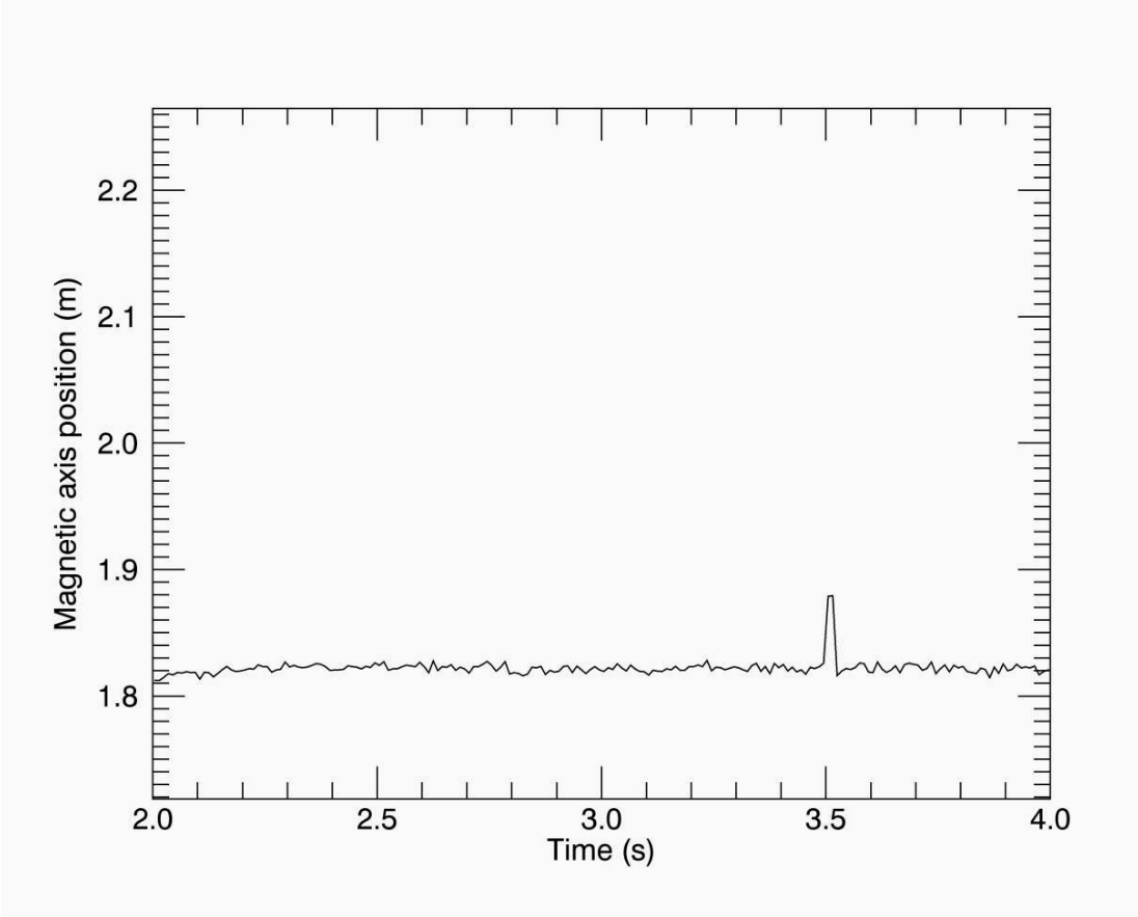

Figure 5. 3: Magnetic axis over time for shot number 13693.

The last and final step of this part of the code development is to obtain the magnetic axis for a specific time.

It is worthy to mention that the same steps are done in two different documents that contain the code to analyse the MSE data. The IDL version for both is different, so slight differences exist between the codes.

5.2. Verification of the results

For the verification of the results of the magnetic axis obtained from MSE data, it is used the *EFIT* code.

First, the magnetic pitch angle from *EFIT* data is uploaded, and as in the same case as when analysing the MSE data, a fitting function is created and the magnetic axis is determined by the point at which the function equals to zero. The code for this case needs to be modified, but keeping in mind the same strategy.

Next, a command is created to be executed automatically to obtain the magnetic axis from the MSE data with the same input parameters set for the *EFIT.*

Finally, the results are compared and plotted in the same graph.

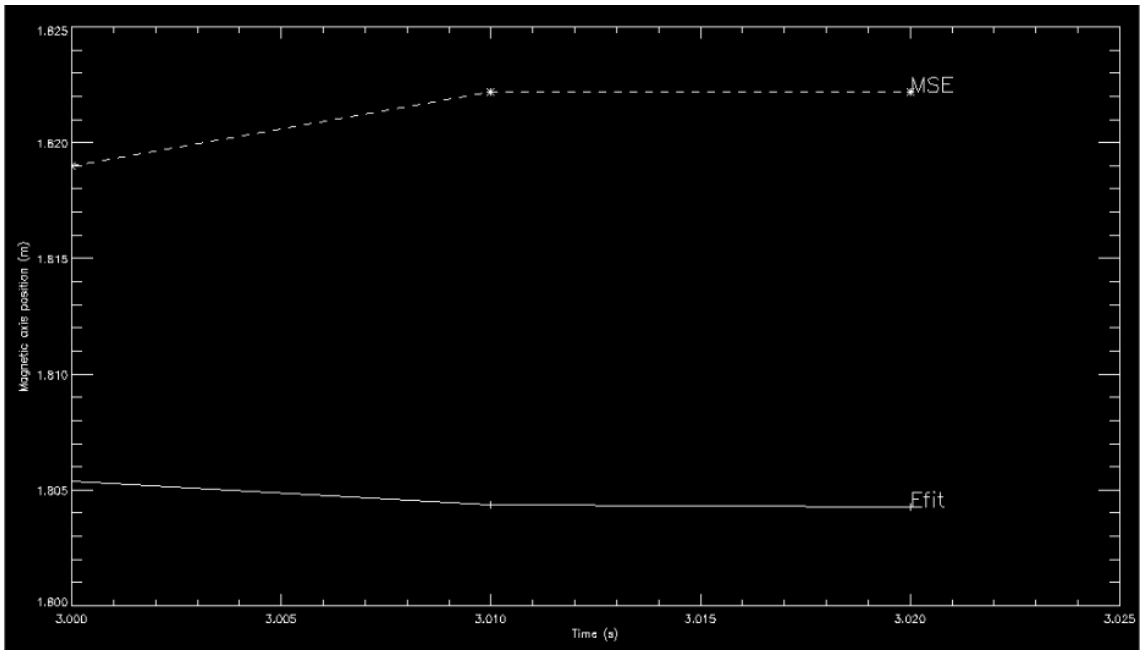

Figure 5. 4: MSE magnetic axis compared with EFIT for shot number 13693 for the times 3.0 s, 3.01 s and 3.02 s.

5.3. Further development

Fusion is a field which needs further development. The principal problem with this technology is the low development level due to its complexity. Hence for sure further development will be performed. On this section some improving ideas are given.

One of the weakest point of this project is the calculation of the error for the magnetic axis obtained from the MSE calculated magnetic pitch angle, hence it will be very interesting to introduce this error in a future version.

A second aspect that may be developed is the verification part, since only two systems are being compared, only knowing which is the expected behaviour and not having the certainty of which of them is the most correct.

6. Results

The results are presented in four groups of four shot each with similar time evolution for both the plasma current and the voltage NBI.

When plotting the magnetic axis over time, the y range of the plot is limited by the radial position of the MSE channels. Hence, in some cases, the resulting plot ma

Finally, for the MSE verification with EFIT, only a small time region is evaluated. In all cases, $\Delta t = 1\ s$ but the beginning time selected is different.

6.1. Plots

Group 1: 13691, 13692, 13693, 13694

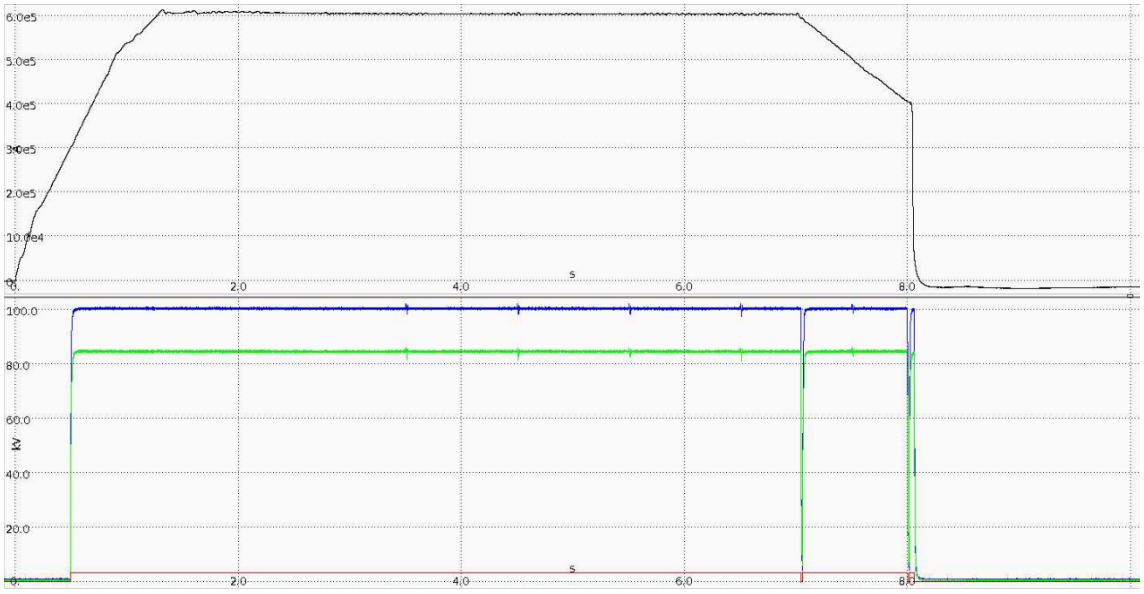

Figure 6. 1: Plasma current (up) and NBI voltage (down), with ION1 blue, ION2 green, ION3 red, for shot 13691.

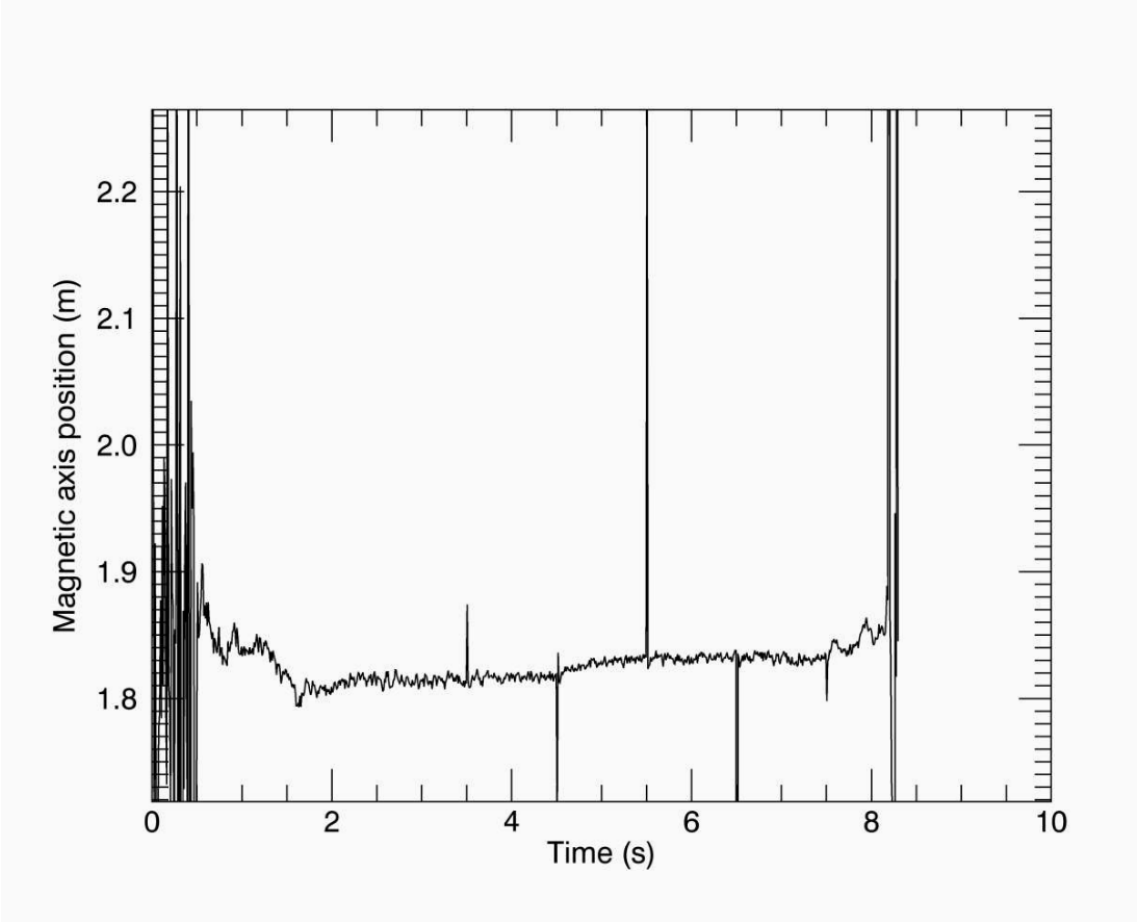

Figure 6. 2: Magnetic axis over time for shot 13691.

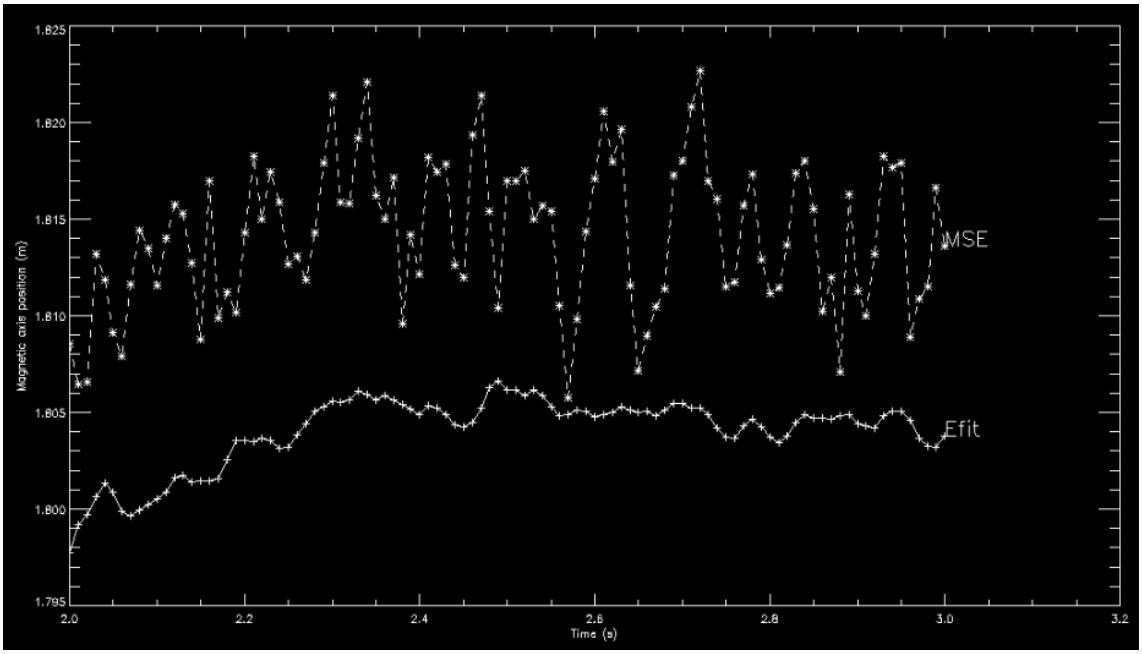

Figure 6. 3: Magnetic axis from MSE and EFIT, over t=2s – 3s for shot 13691.

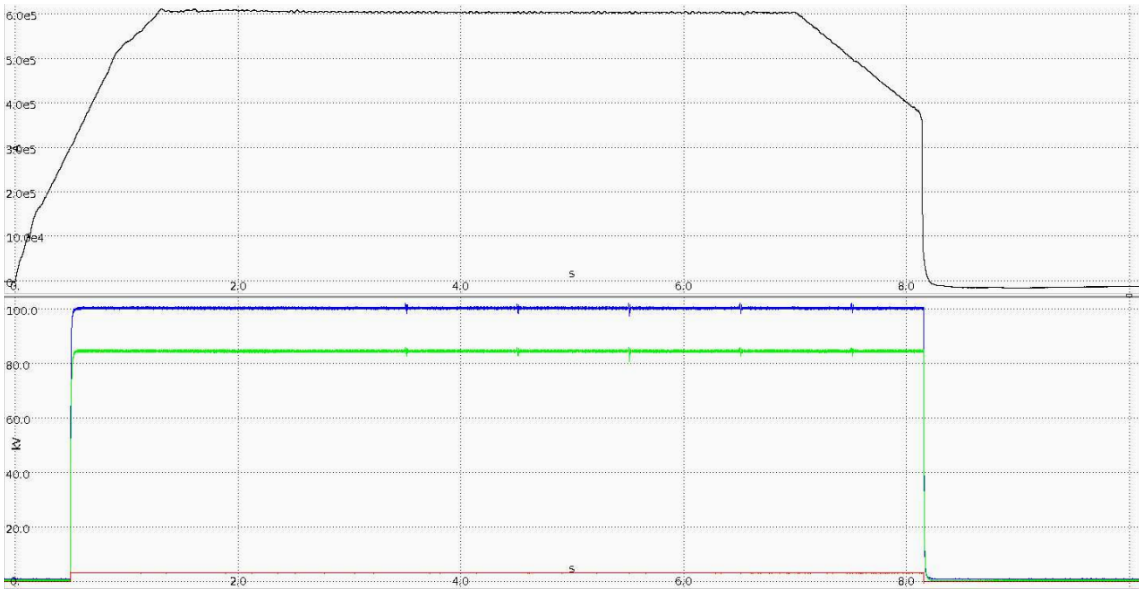

Figure 6. 4: Plasma current (up) and NBI voltage (down), with ION1 blue, ION2 green, ION3 red, for shot 13692.

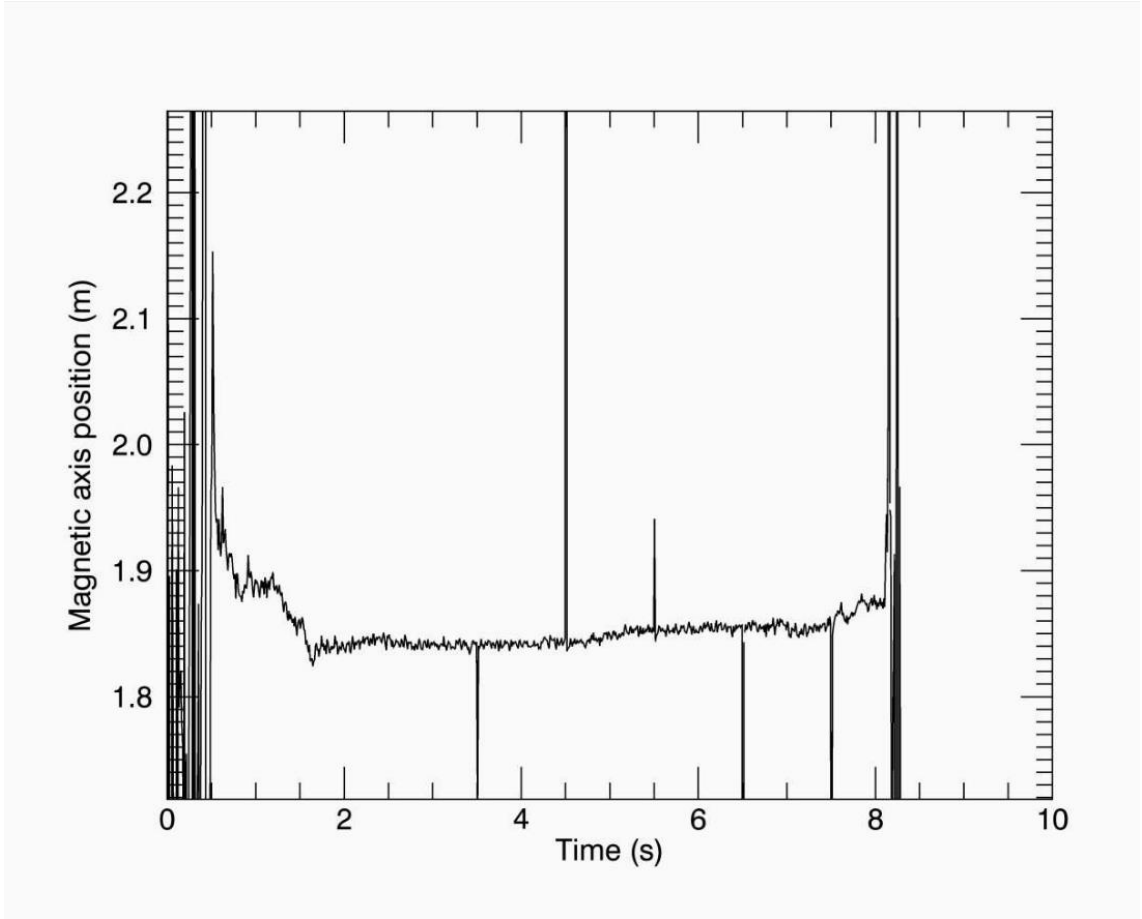

Figure 6. 5: Magnetic axis over time for shot 13692.

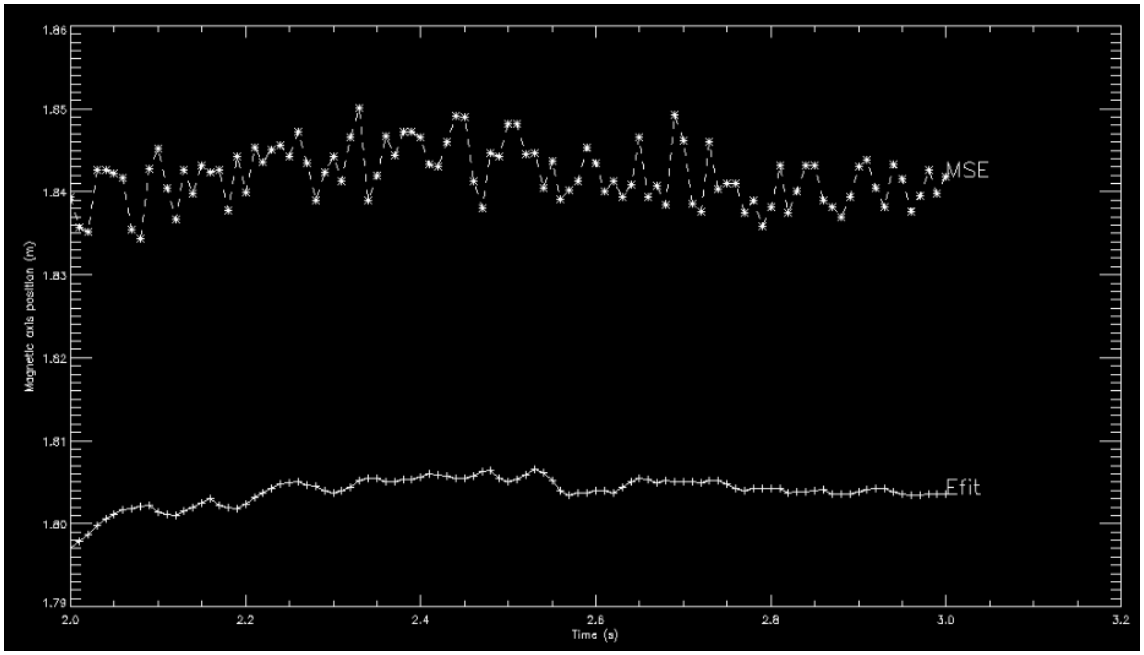

Figure 6. 6: Magnetic axis from MSE and EFIT, over t=2s – 3s for shot 13692.

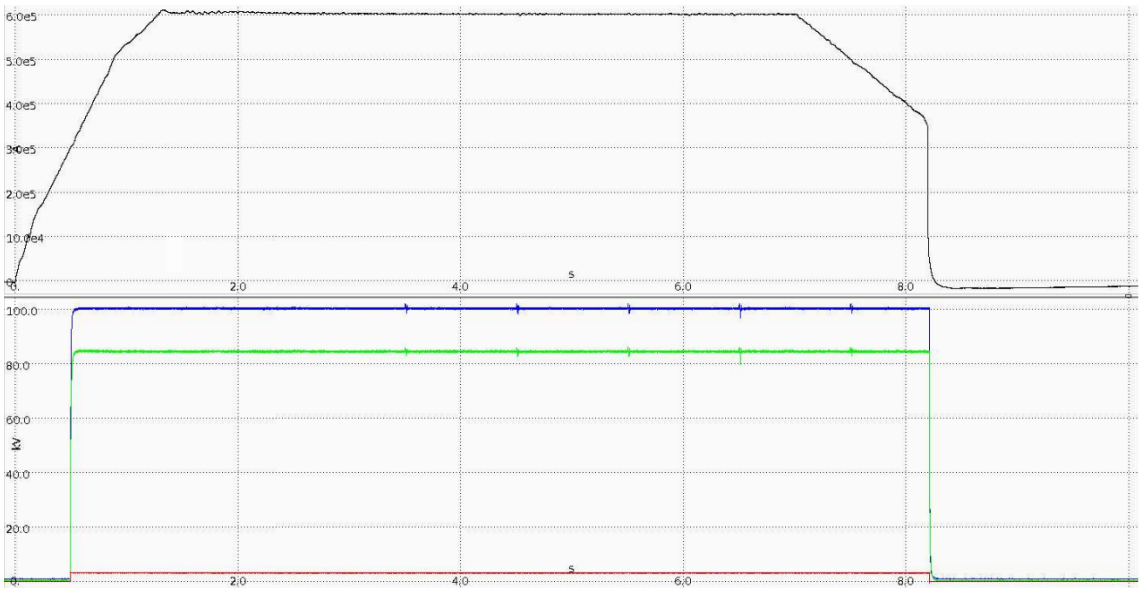

Figure 6. 7: Plasma current (up) and NBI voltage (down), with ION1 blue, ION2 green, ION3 red, for shot 13693.

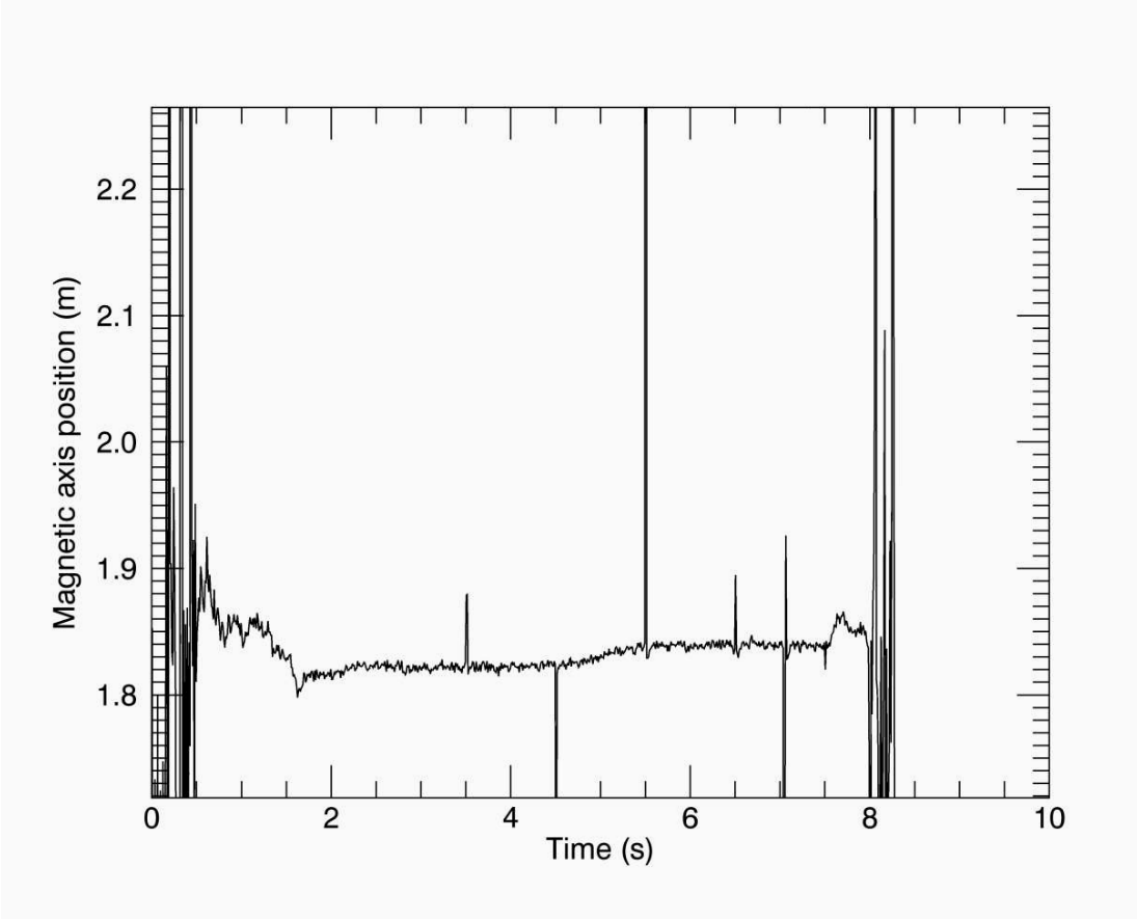

Figure 6. 8: Magnetic axis over time for shot 13693

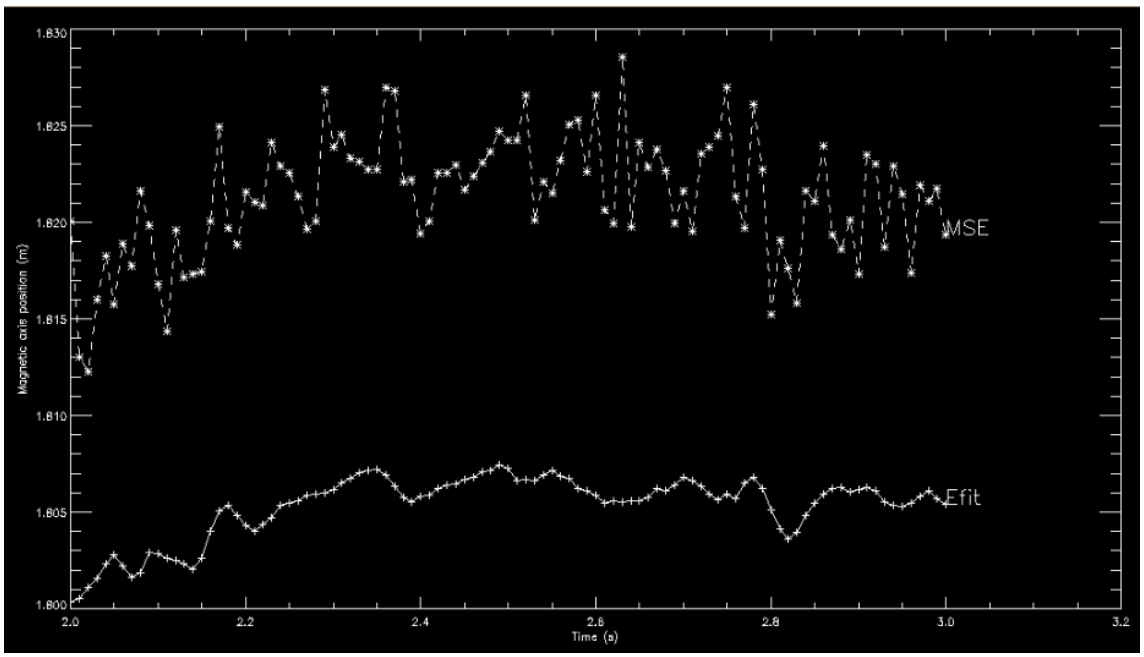

Figure 6. 9: Magnetic axis from MSE and EFIT, over t=2s – 3s for shot 13693.

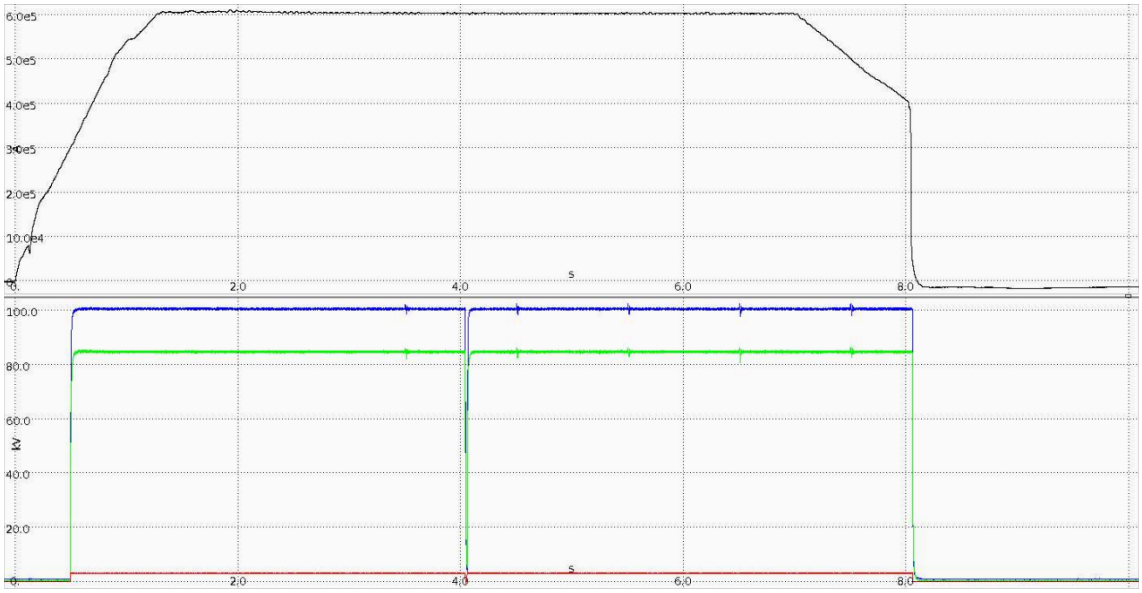

Figure 6. 10: Plasma current (up) and NBI voltage (down), with ION1 blue, ION2 green, ION3 red, for shot 13694.

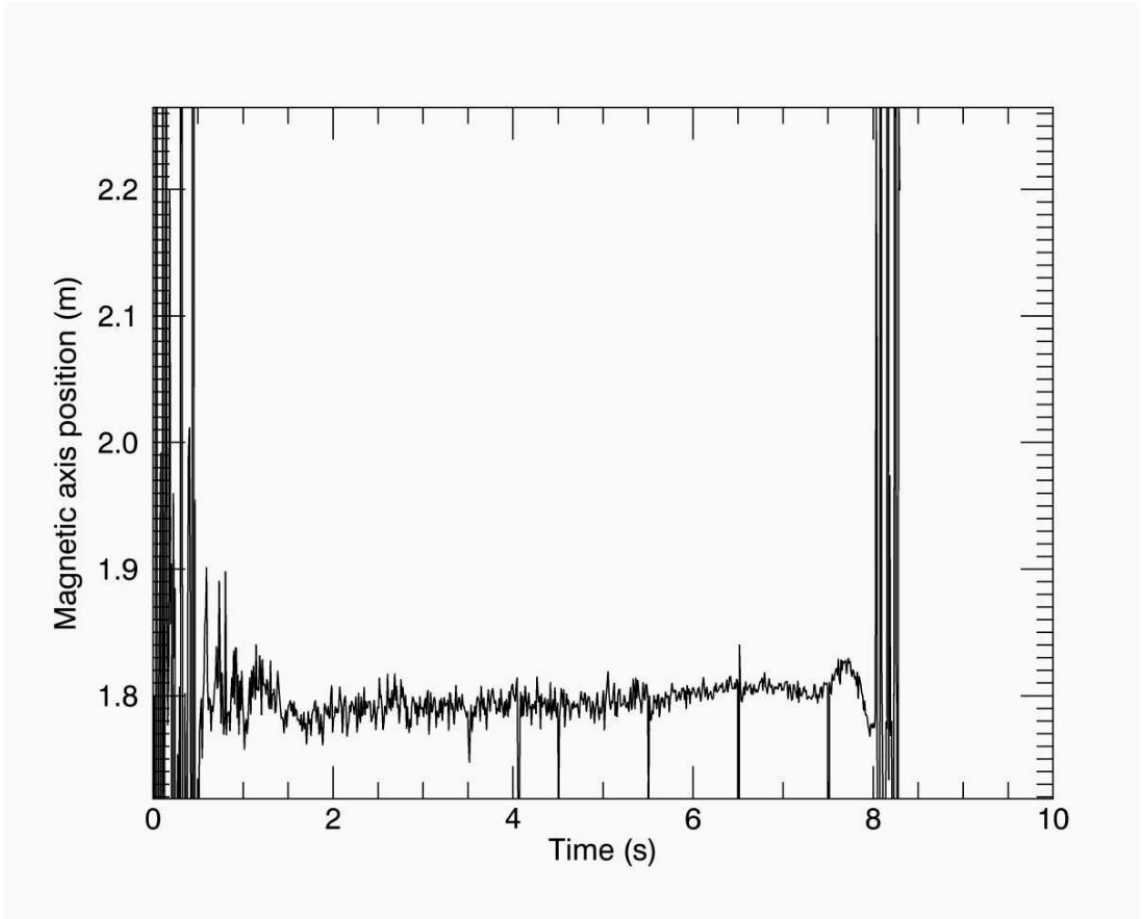

Figure 6. 11: Magnetic axis over time for shot 13694

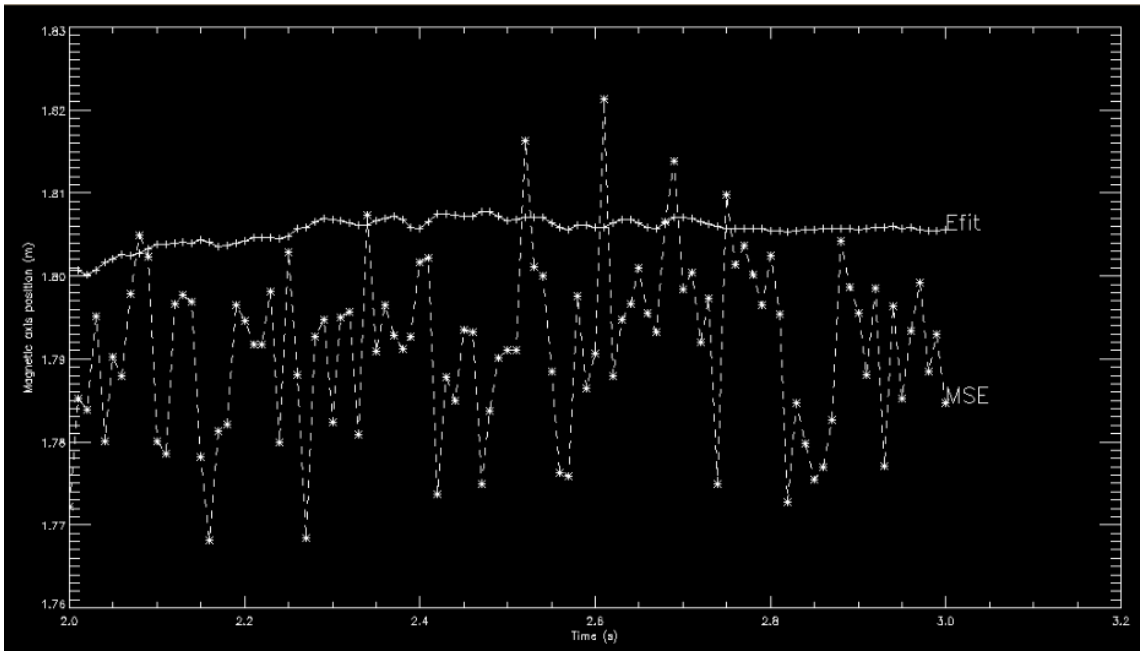

Figure 6. 12: Magnetic axis from MSE and EFIT, over t=2s – 3s for shot 13694.

Group 2: 13724, 13725, 13727, 13728

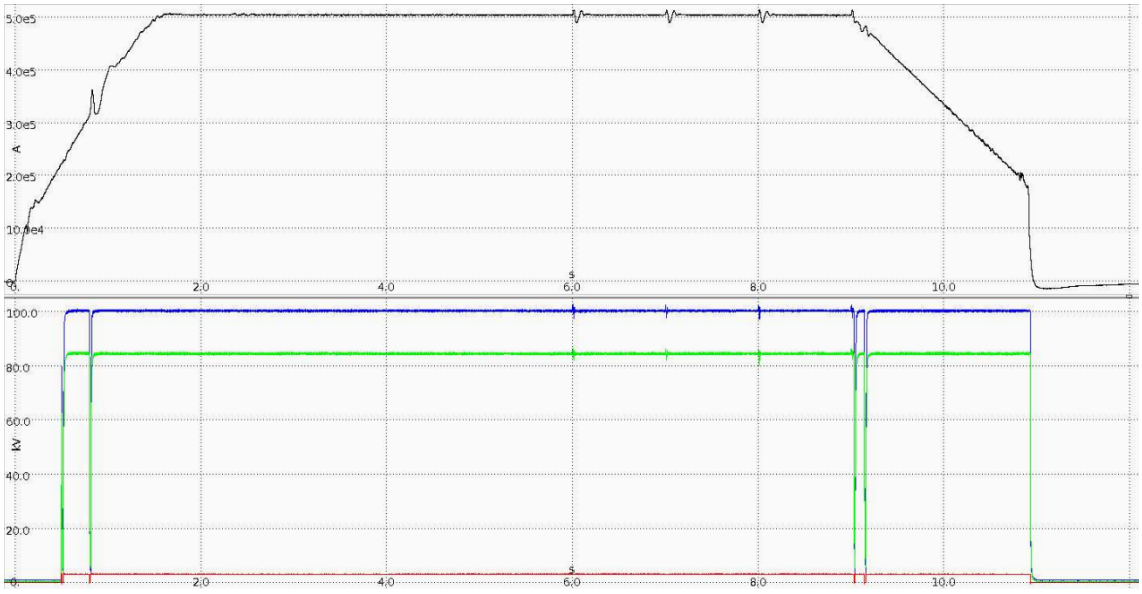

Figure 6. 13: Plasma current (up) and NBI voltage (down), with ION1 blue, ION2 green, ION3 red, for shot 13724.

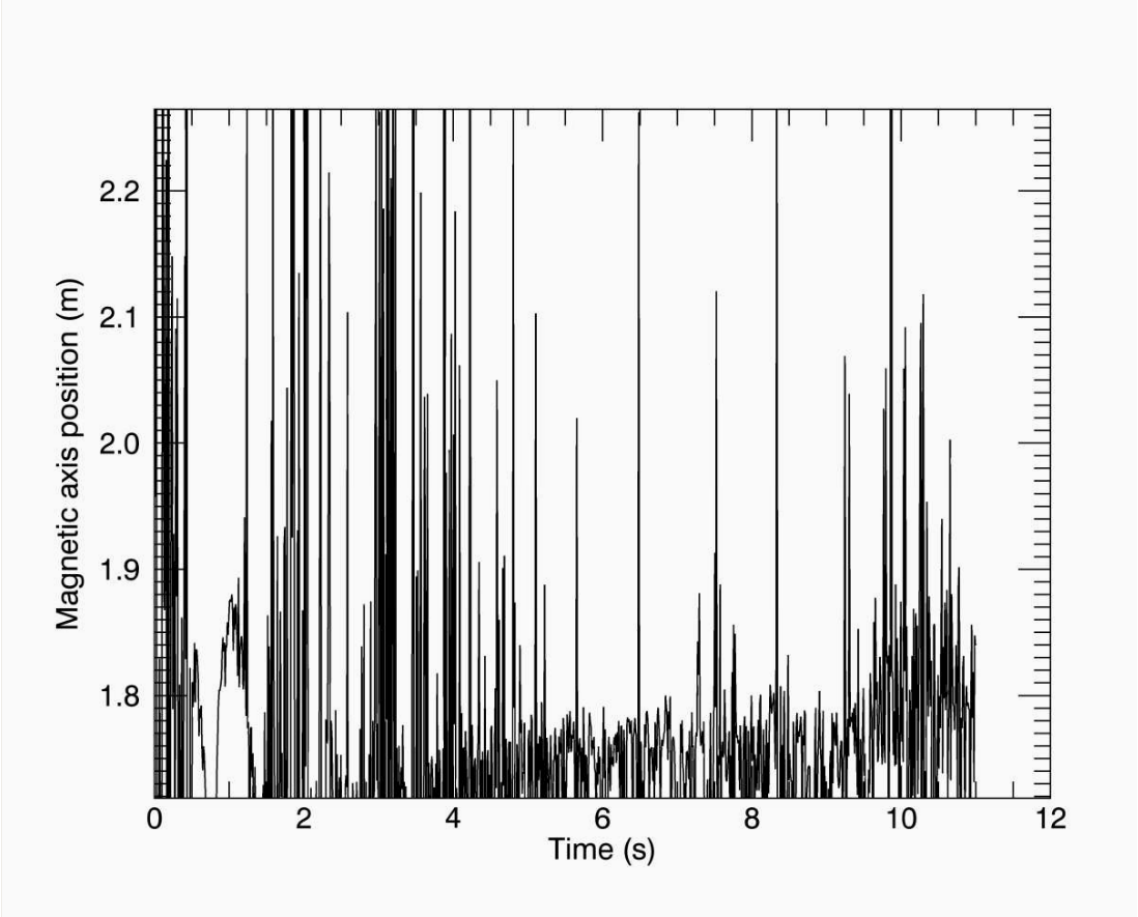

Figure 6. 14: Magnetic axis over time for shot 13724.

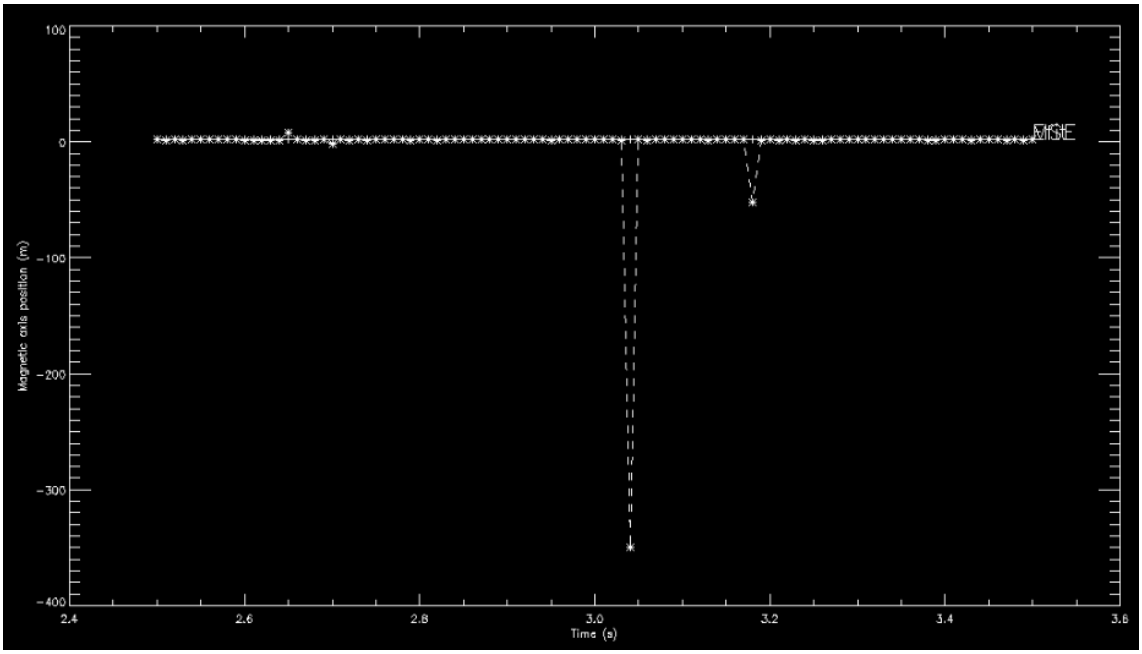

Figure 6. 15: Magnetic axis from MSE and EFIT, over t=2.5s – 3.5s for shot 13724.

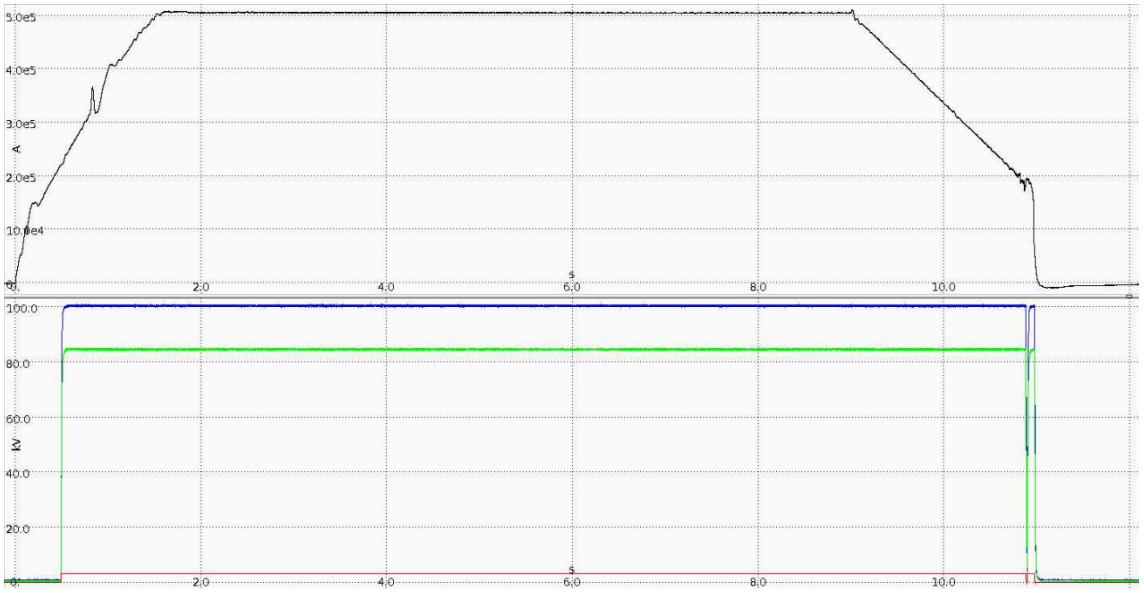

Figure 6. 16: Plasma current (up) and NBI voltage (down), with ION1 blue, ION2 green, ION3 red, for shot 13725.

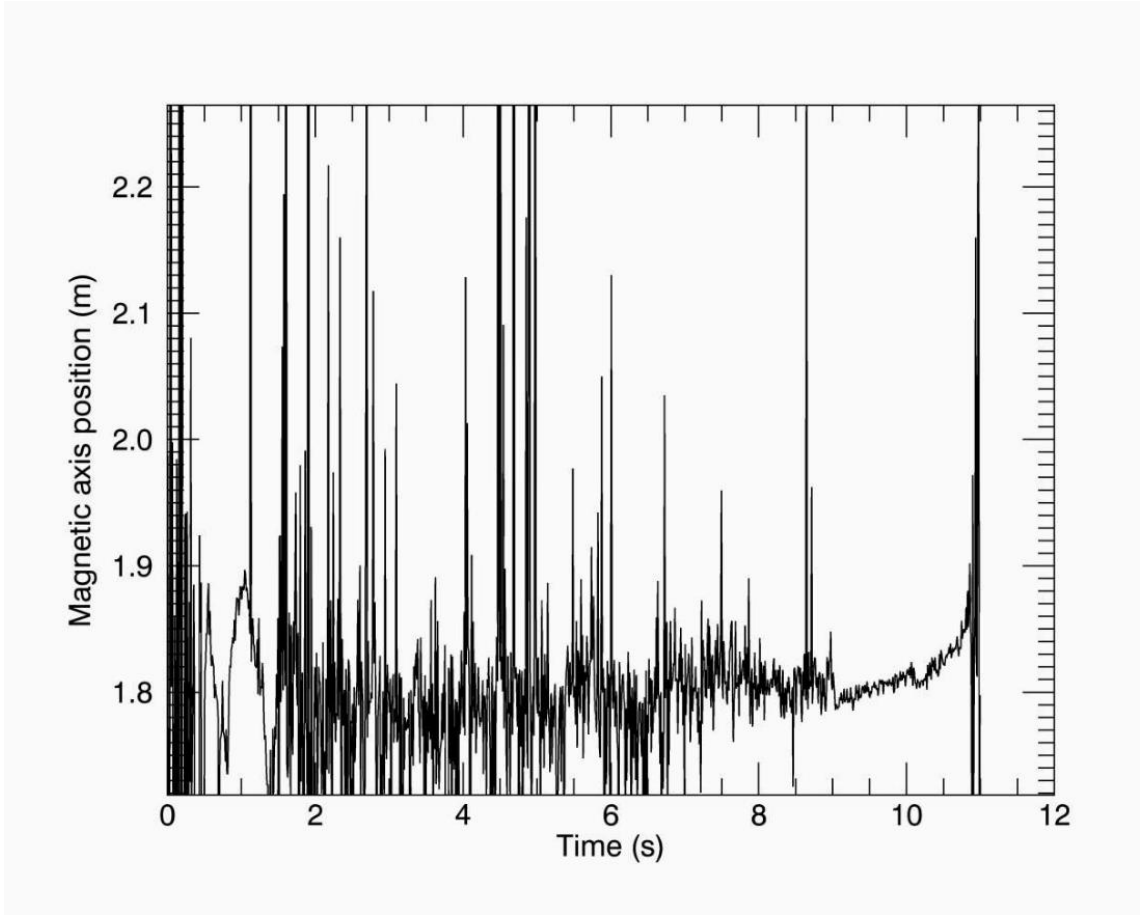

Figure 6. 17: Magnetic axis over time for shot 13725.

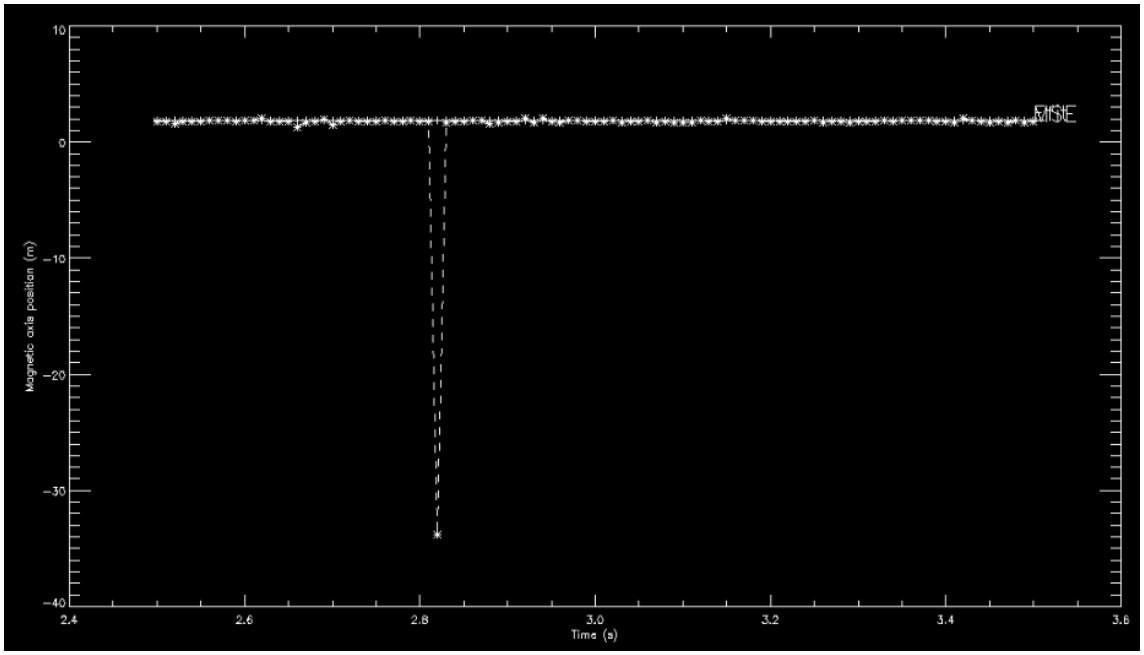

Figure 6. 18 Magnetic axis from MSE and EFIT, over t=2.5s – 3.5s for shot 13725.

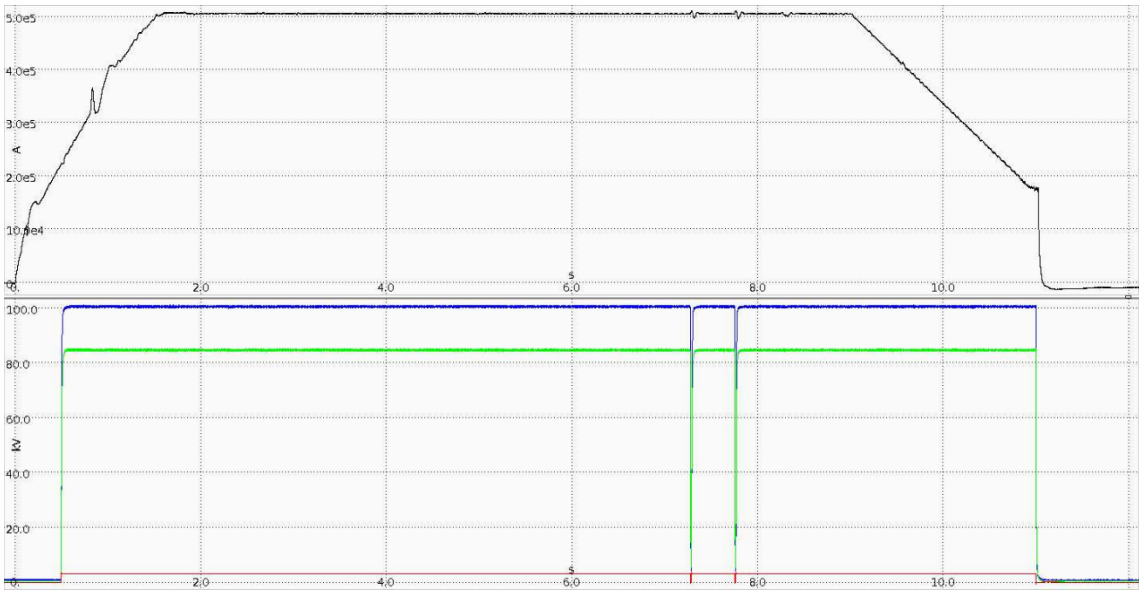

Figure 6. 19: Plasma current (up) and NBI voltage (down), with ION1 blue, ION2 green, ION3 red, for shot 13727.

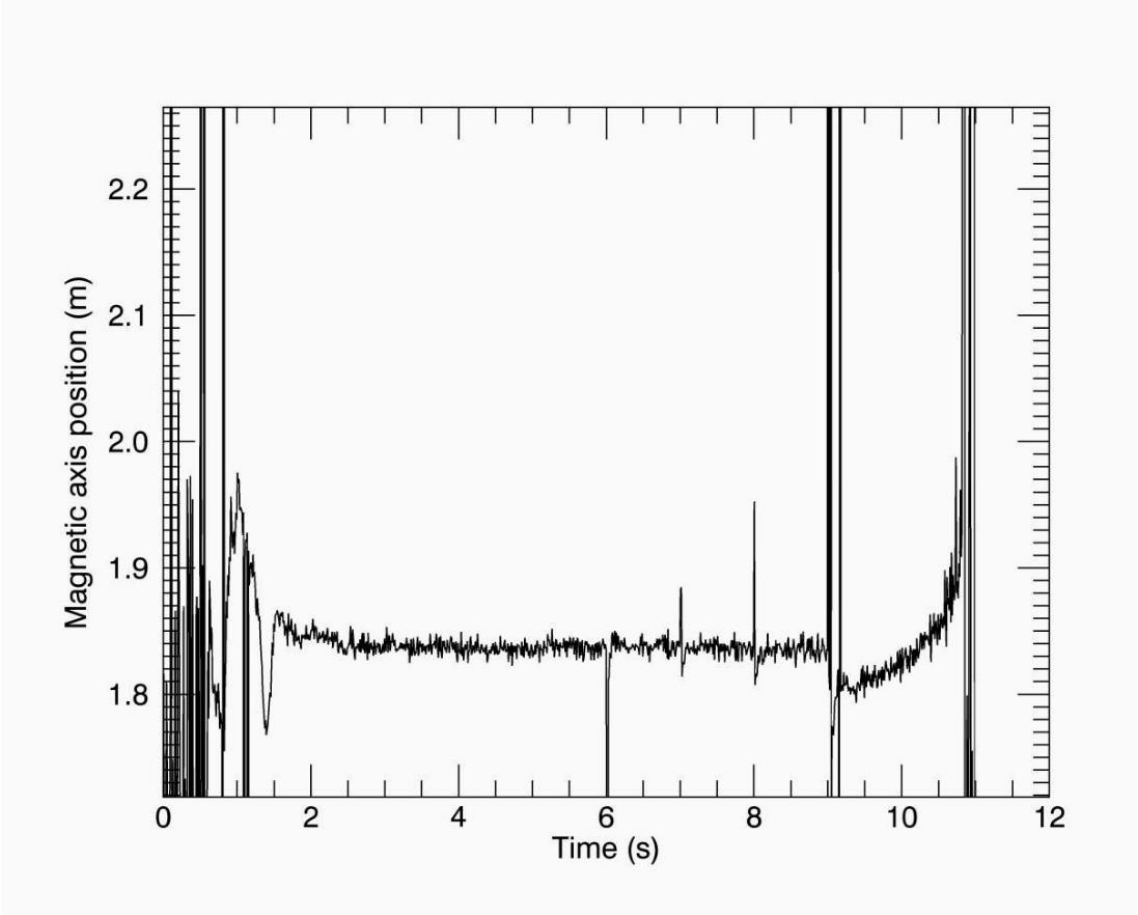

Figure 6. 20: Magnetic axis over time for shot 13727.

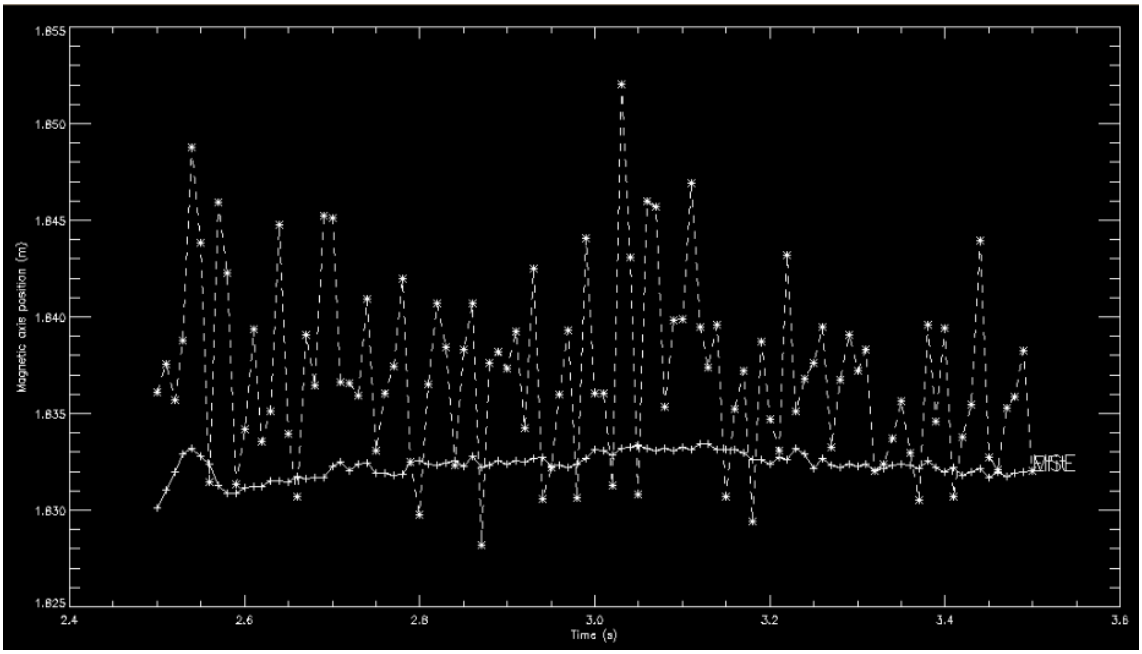

Figure 6. 21: Magnetic axis from MSE and EFIT, over t=2.5s – 3.5s for shot 13727.

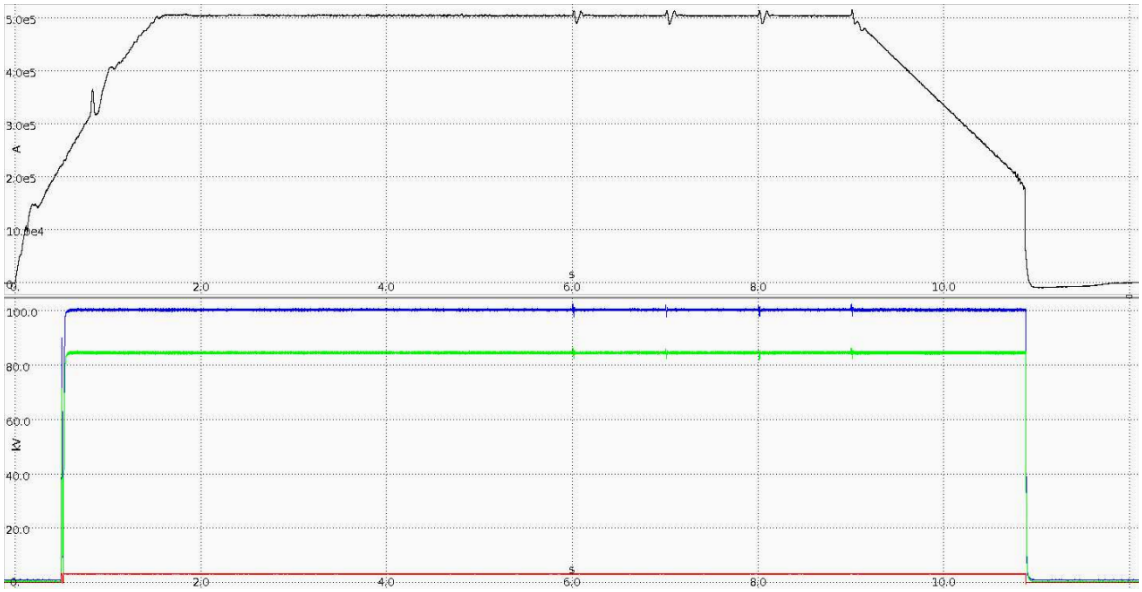

Figure 6. 22: Plasma current (up) and NBI voltage (down), with ION1 blue, ION2 green, ION3 red, for shot 13728.

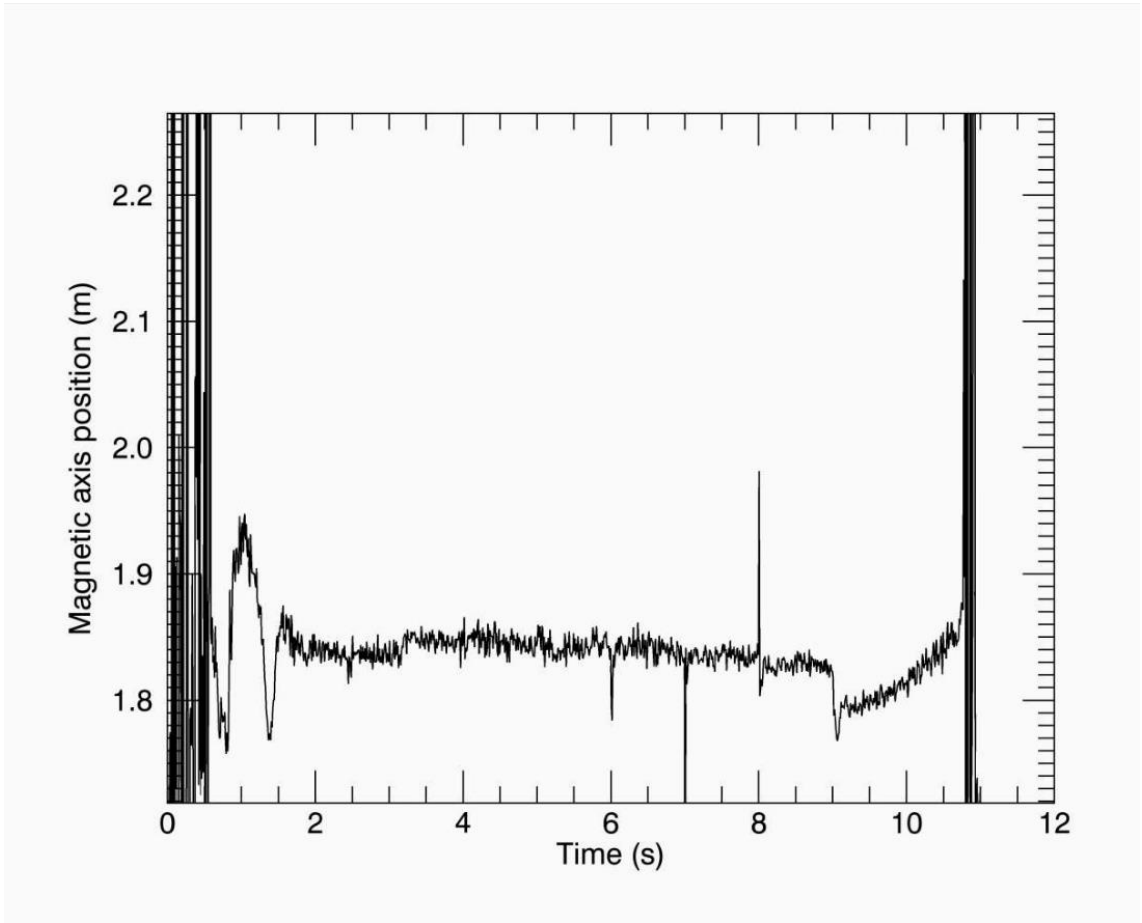

Figure 6. 23: Magnetic axis over time for shot 13728

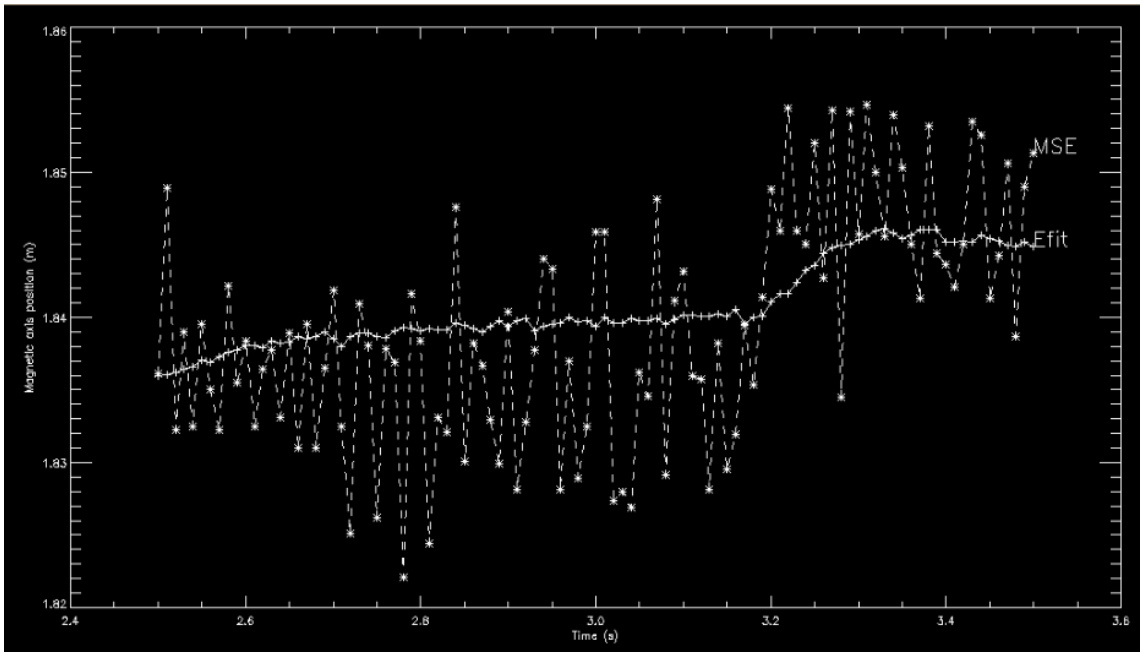

Figure 6. 24: Magnetic axis from MSE and EFIT, over t=2.5s – 3.5s for shot 13728.

Group 3: 13903, 13904, 13905, 13906

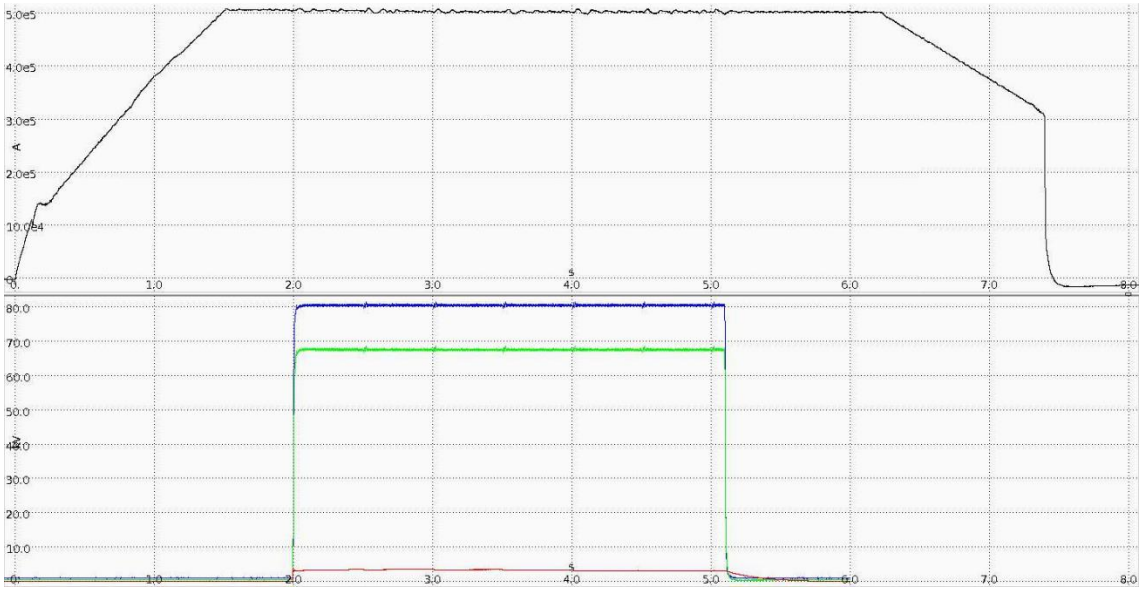

Figure 6. 25: Plasma current (up) and NBI voltage (down), with ION1 blue, ION2 green, ION3 red, for shot 13903.

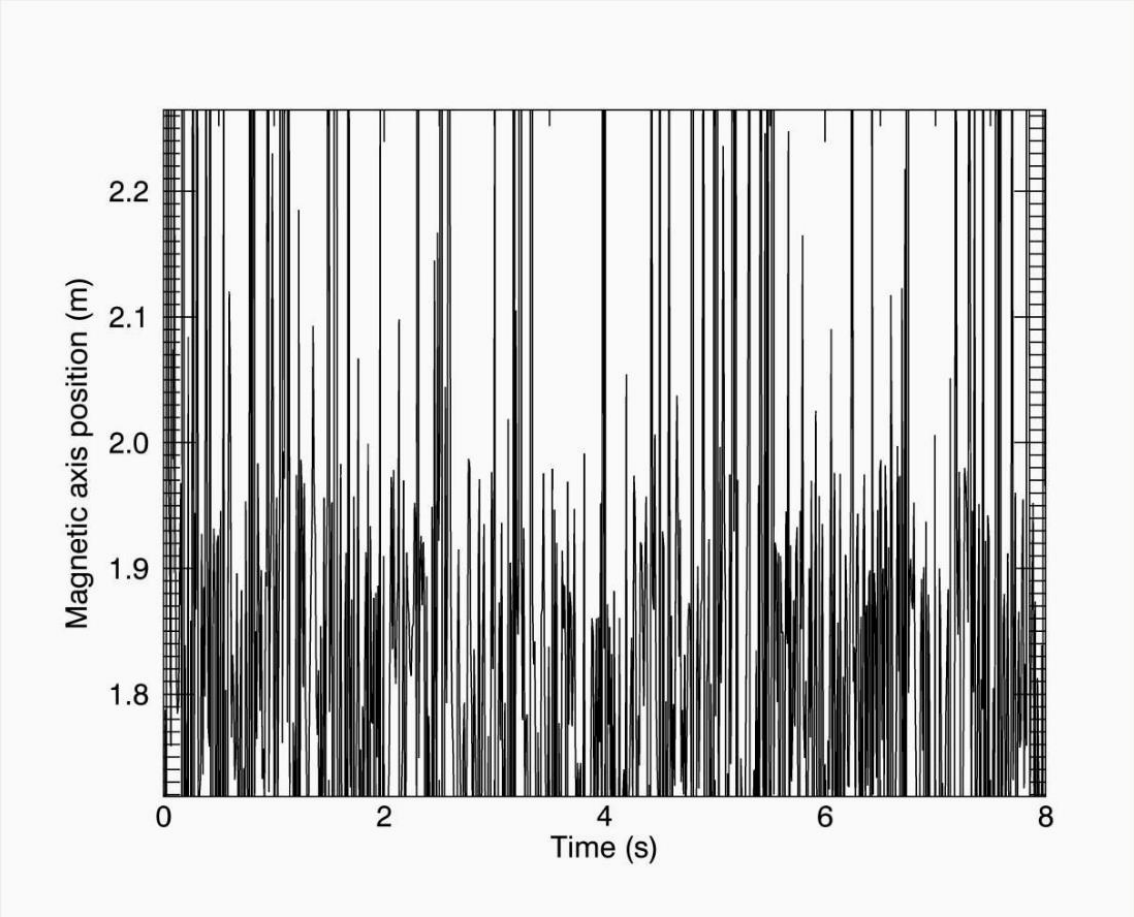

Figure 6. 26: Magnetic axis over time for shot 13903.

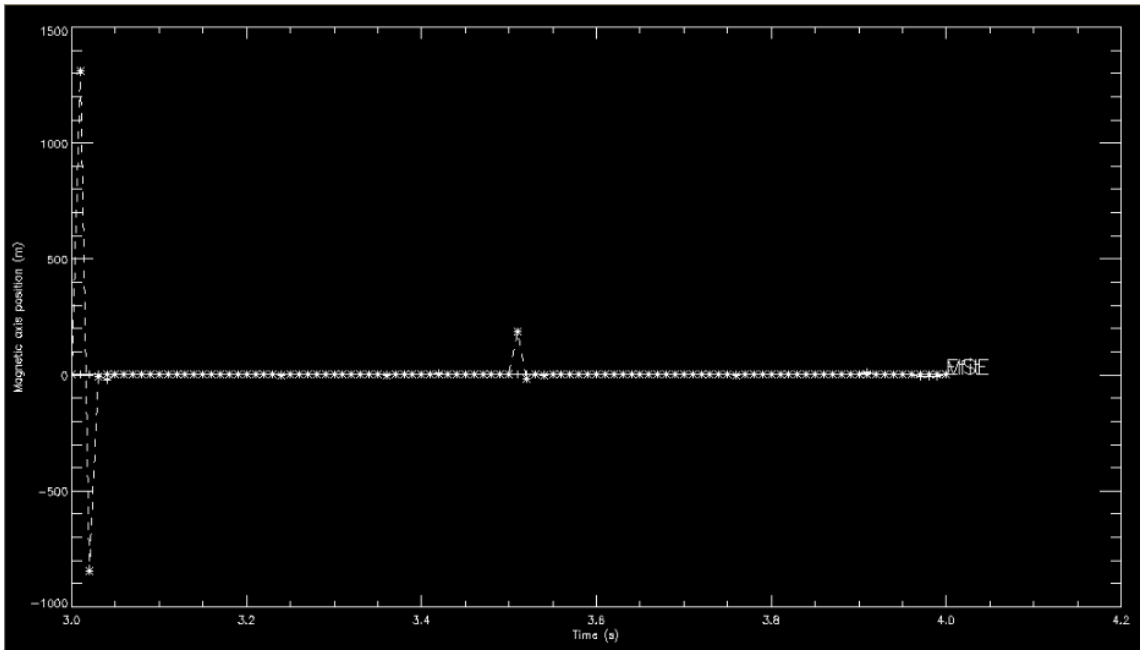

Figure 6. 27: Magnetic axis from MSE and EFIT, over t=3s – 4s for shot 13903.

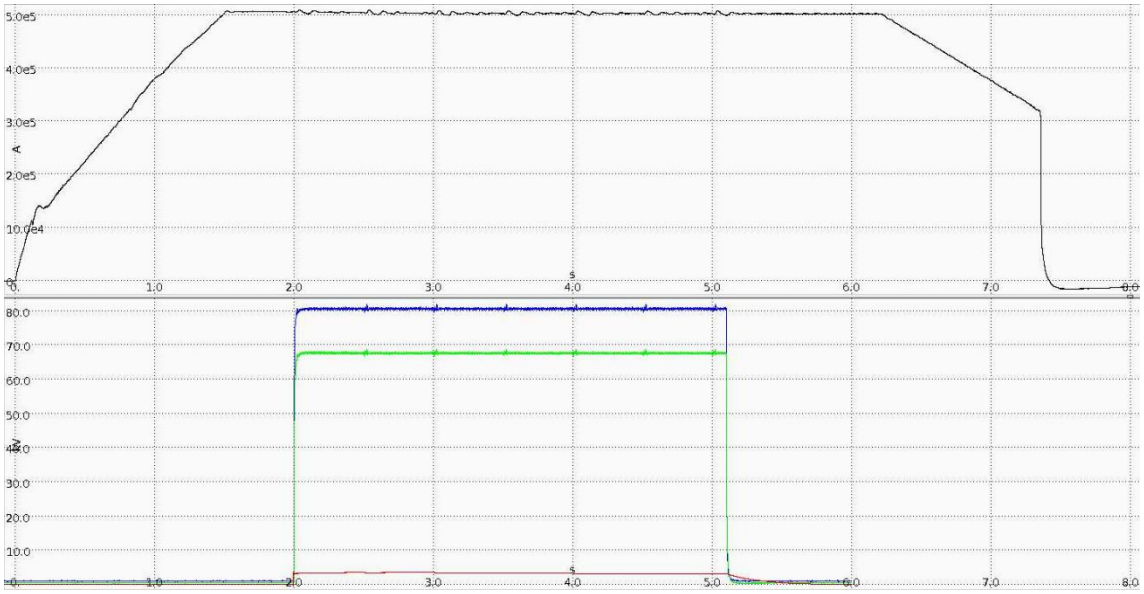

Figure 6. 28: Plasma current (up) and NBI voltage (down), with ION1 blue, ION2 green, ION3 red, for shot 13904.

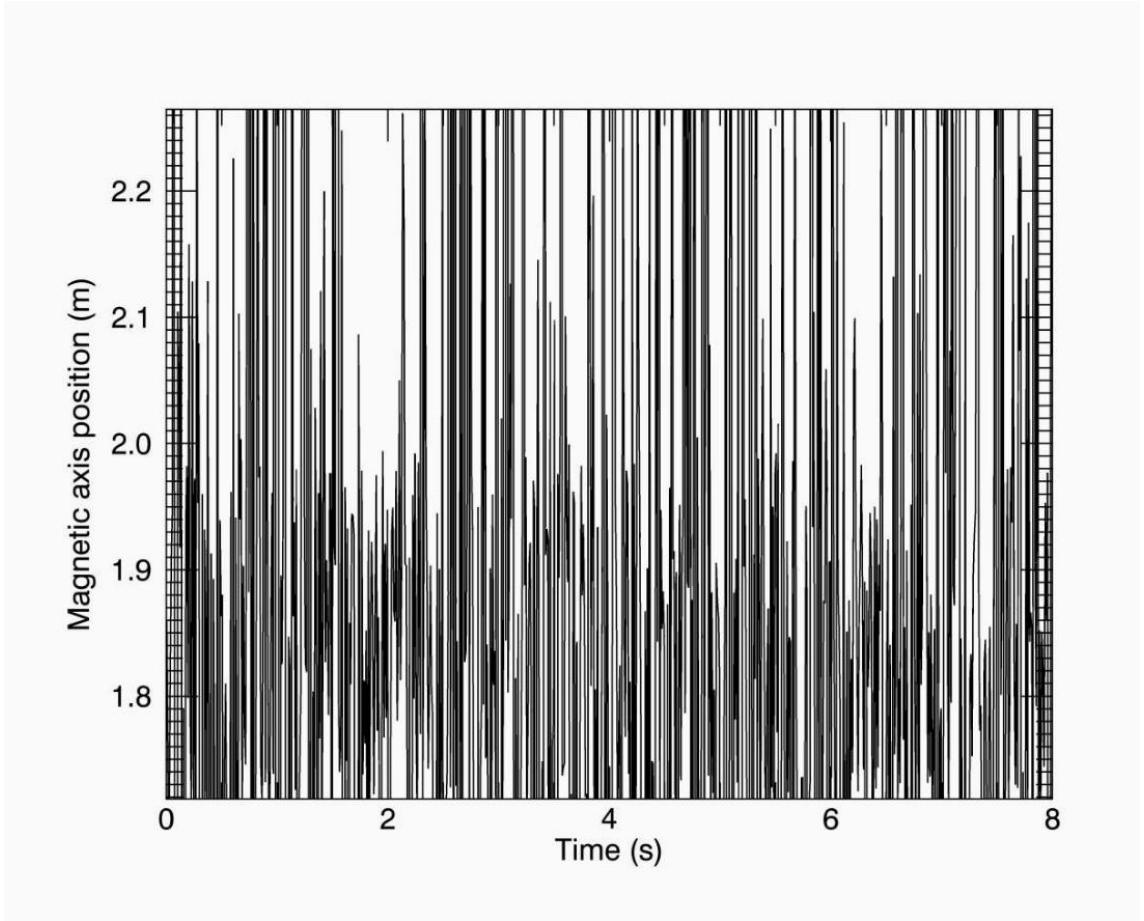

Figure 6. 29: Magnetic axis over time for shot 13904.

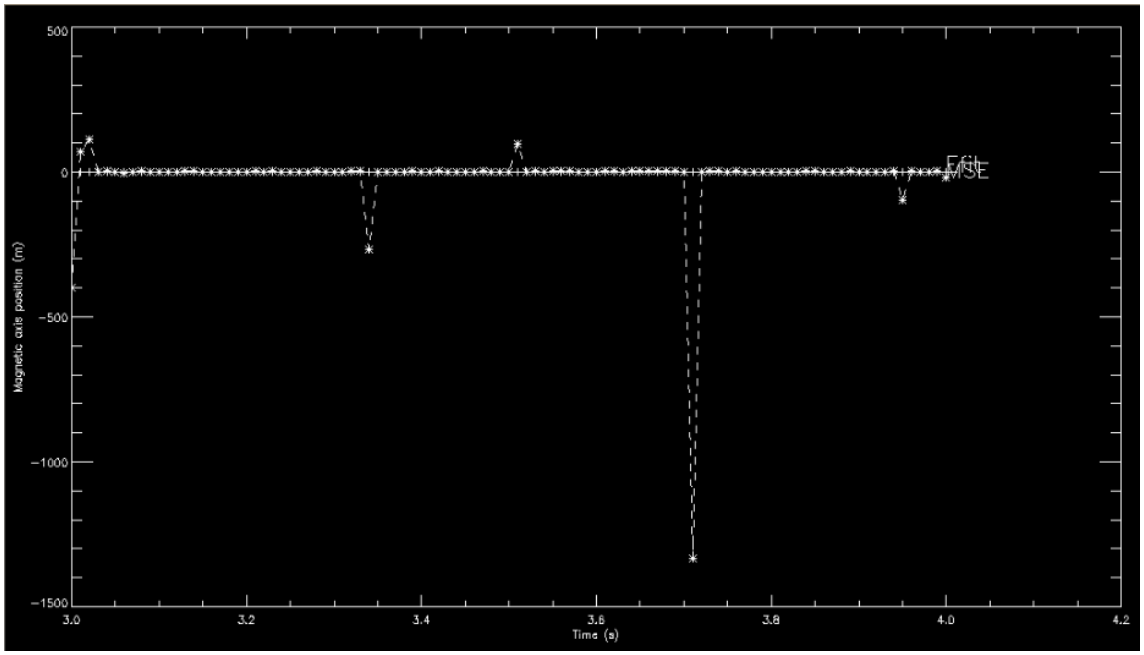

Figure 6. 30: : Magnetic axis from MSE and EFIT, over t=3s – 4s for shot 13904.

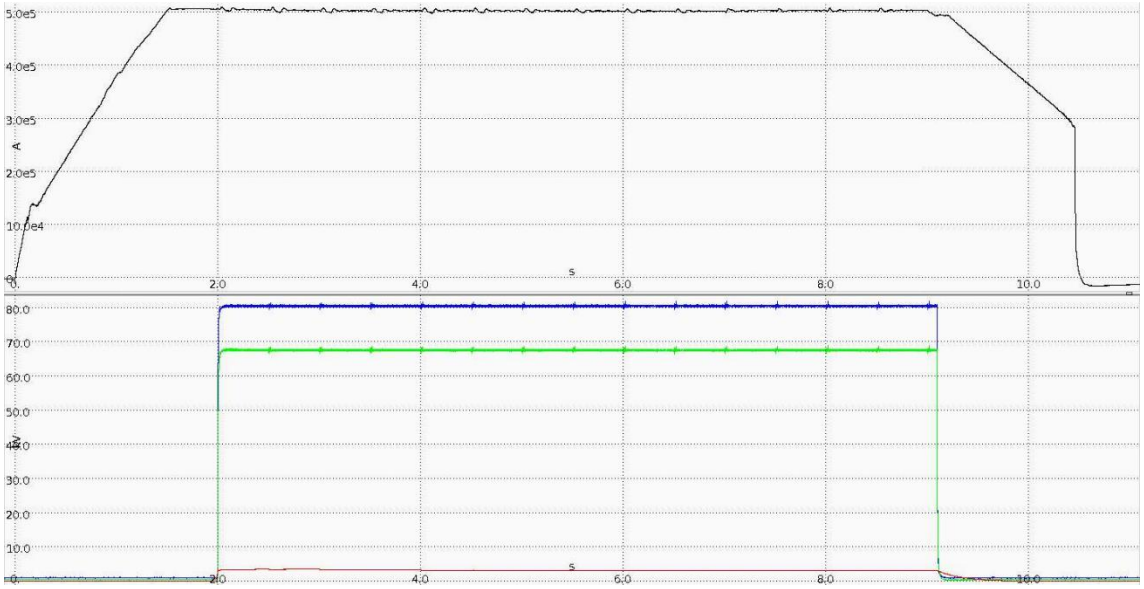

Figure 6. 31: Plasma current (up) and NBI voltage (down), with ION1 blue, ION2 green, ION3 red, for shot 13905.

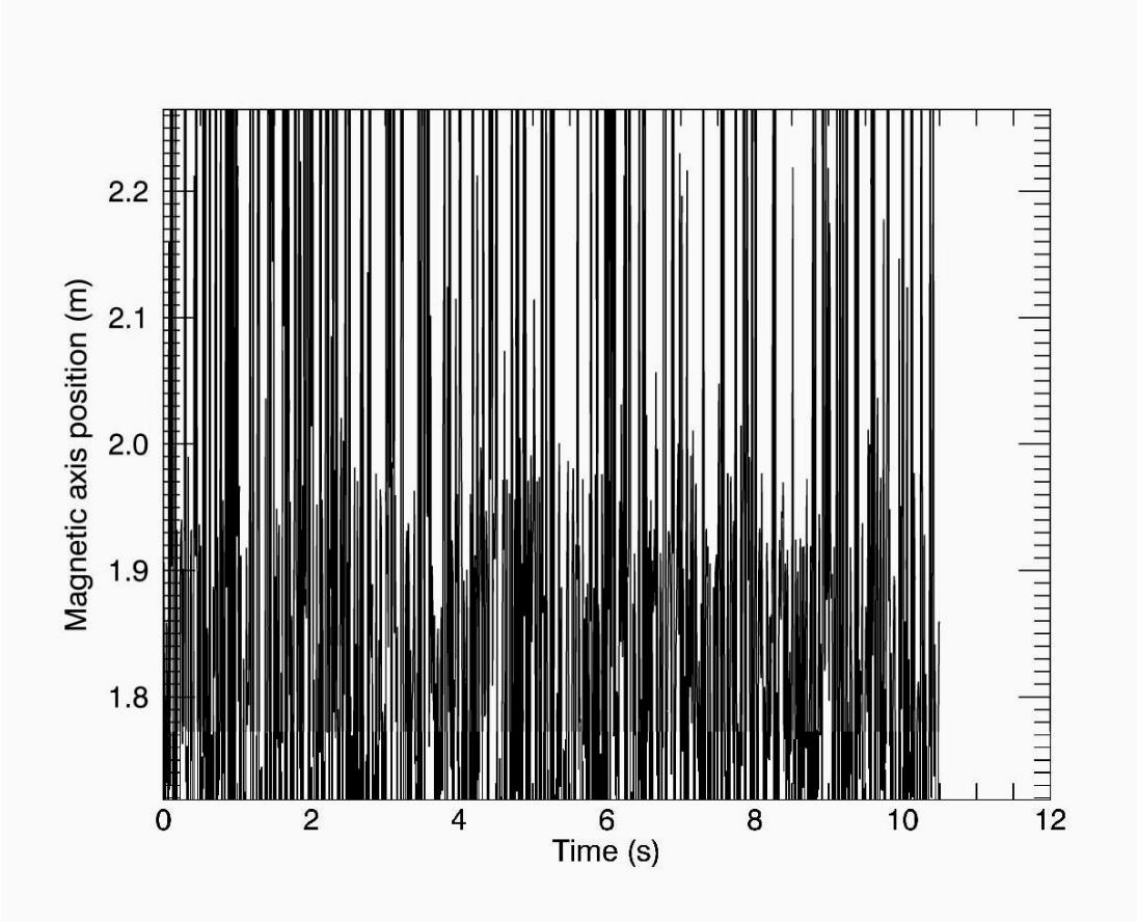

Figure 6. 32: Magnetic axis over time for shot 13905.

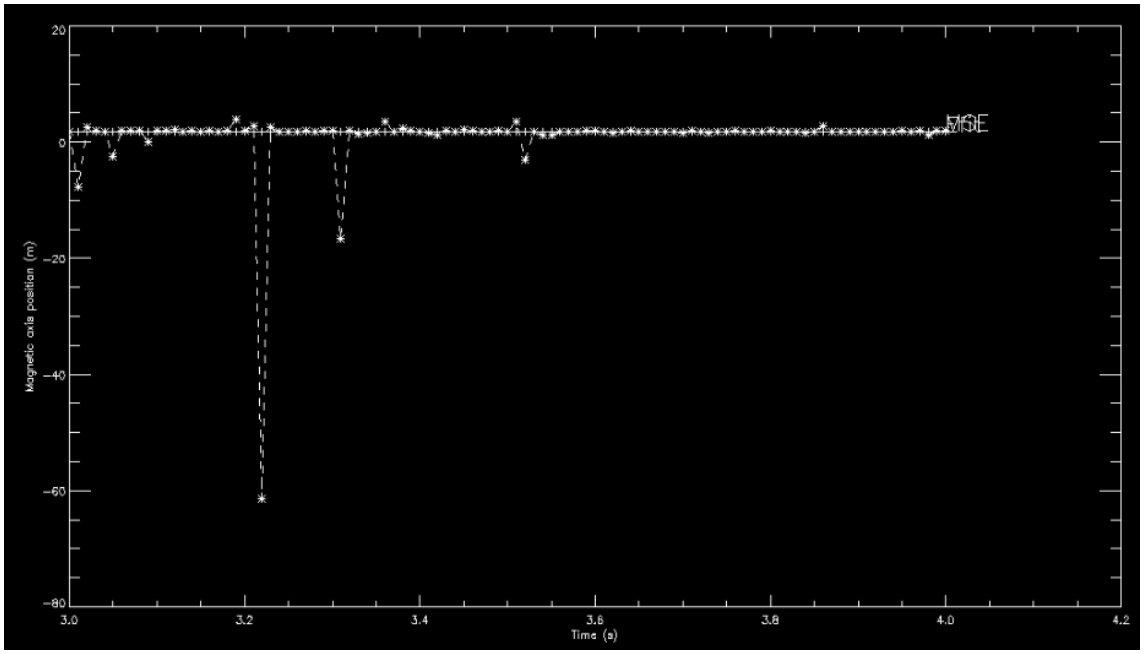

Figure 6. 33: Magnetic axis from MSE and EFIT, over t=3s – 4s for shot 13905.

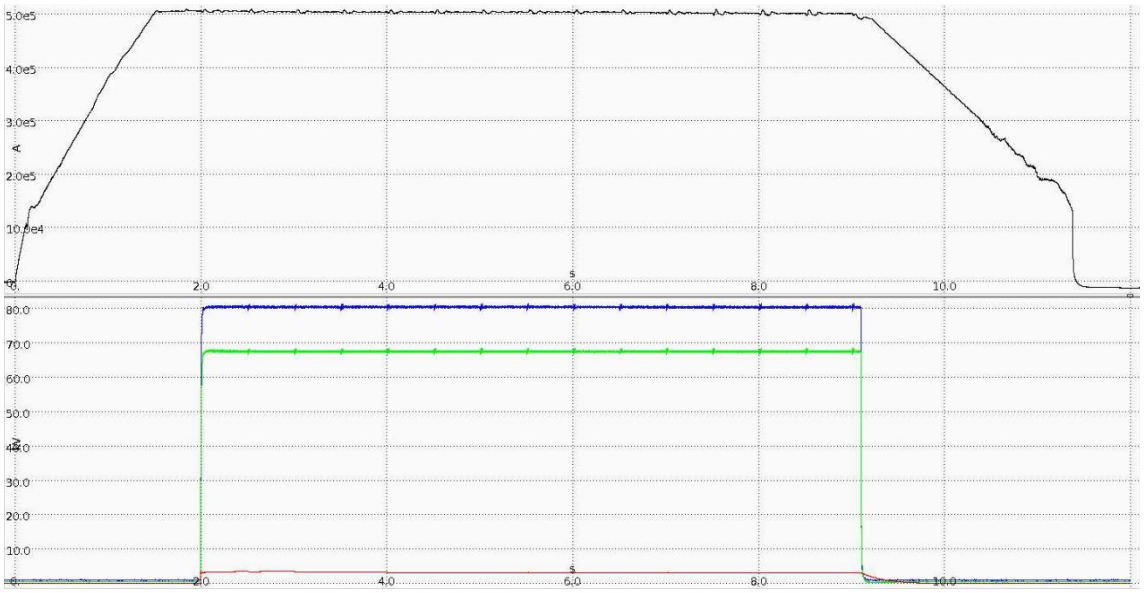

Figure 6. 34: Plasma current (up) and NBI voltage (down), with ION1 blue, ION2 green, ION3 red, for shot 13906.

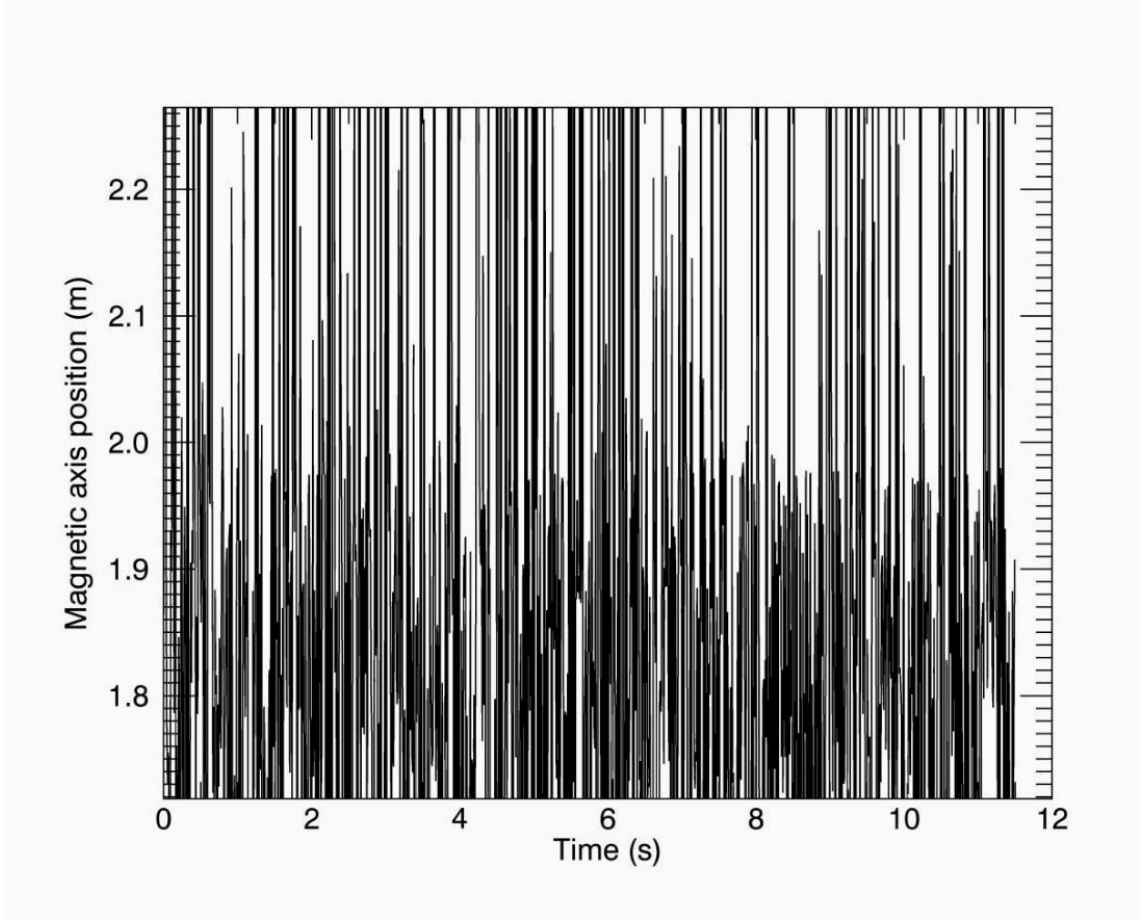

Figure 6. 35: Magnetic axis over time for shot 13906.

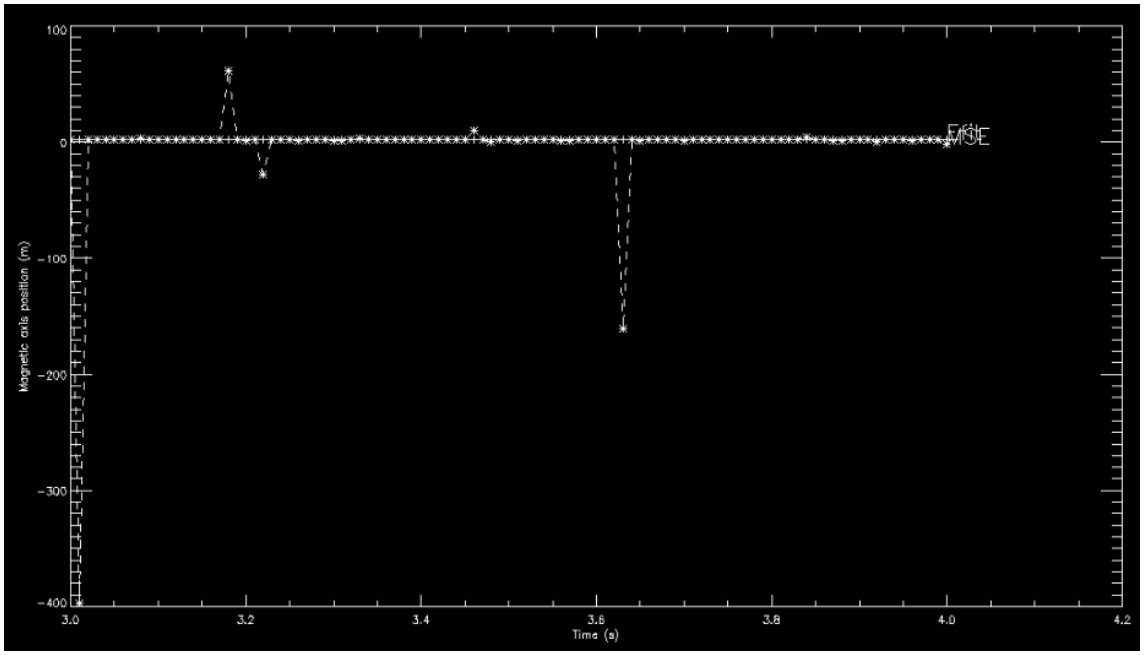

Figure 6. 36: Magnetic axis from MSE and EFIT, over t=3s – 4s for shot 13906.

Group 4: 14202, 14203, 14204, 14205

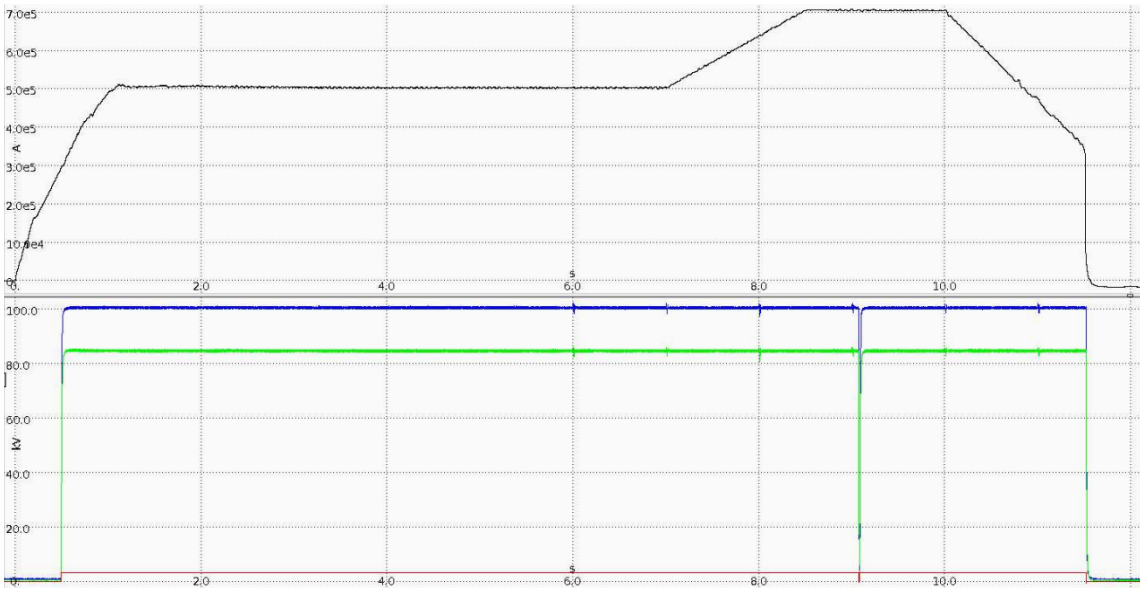

Figure 6. 37: Plasma current (up) and NBI voltage (down), with ION1 blue, ION2 green, ION3 red, for shot 14202.

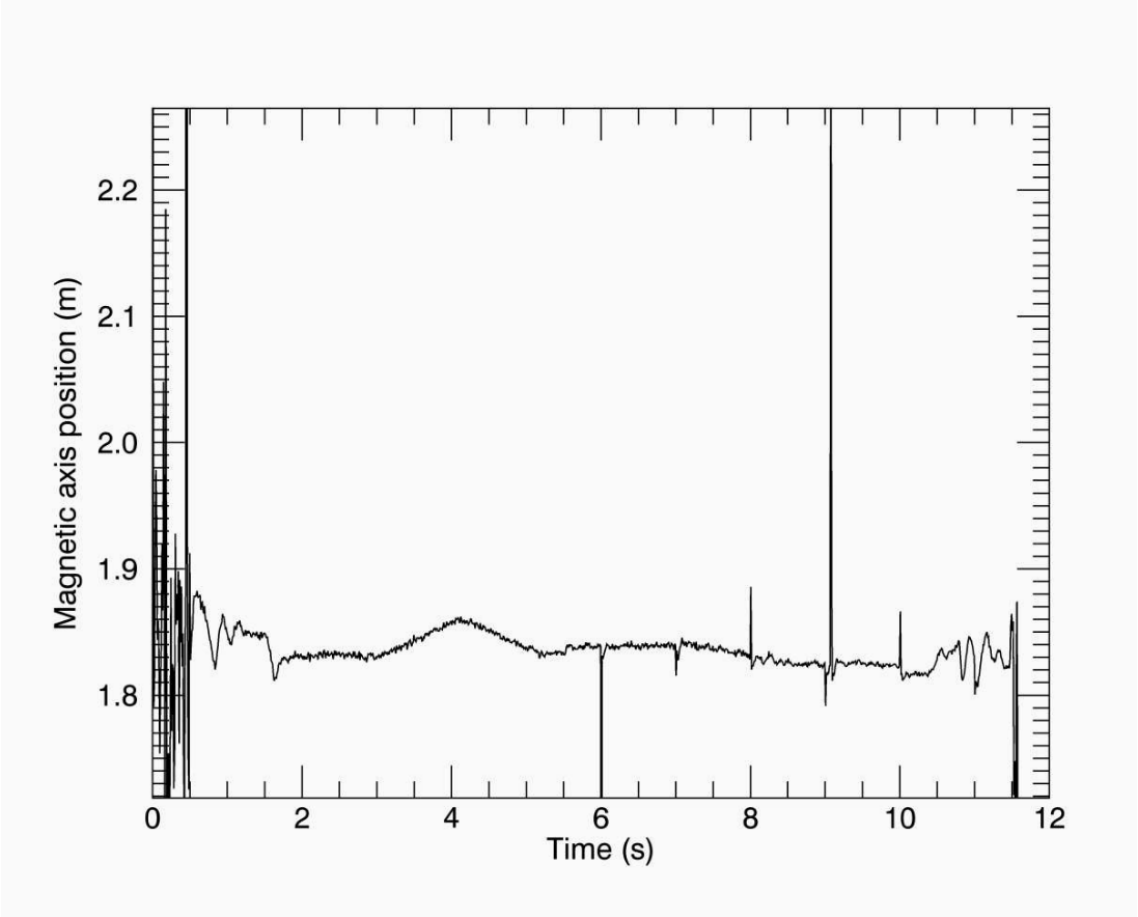

Figure 6. 38: Magnetic axis over time for shot 14202.

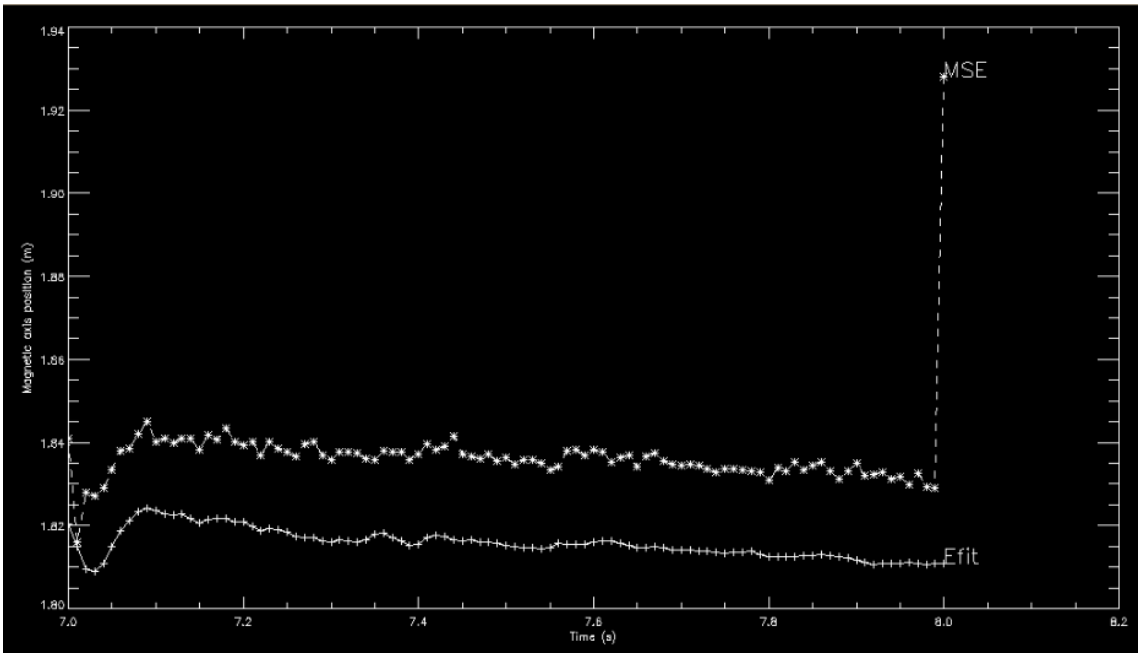

Figure 6. 39: Magnetic axis from MSE and EFIT, over t=7s – 8s for shot 14202.

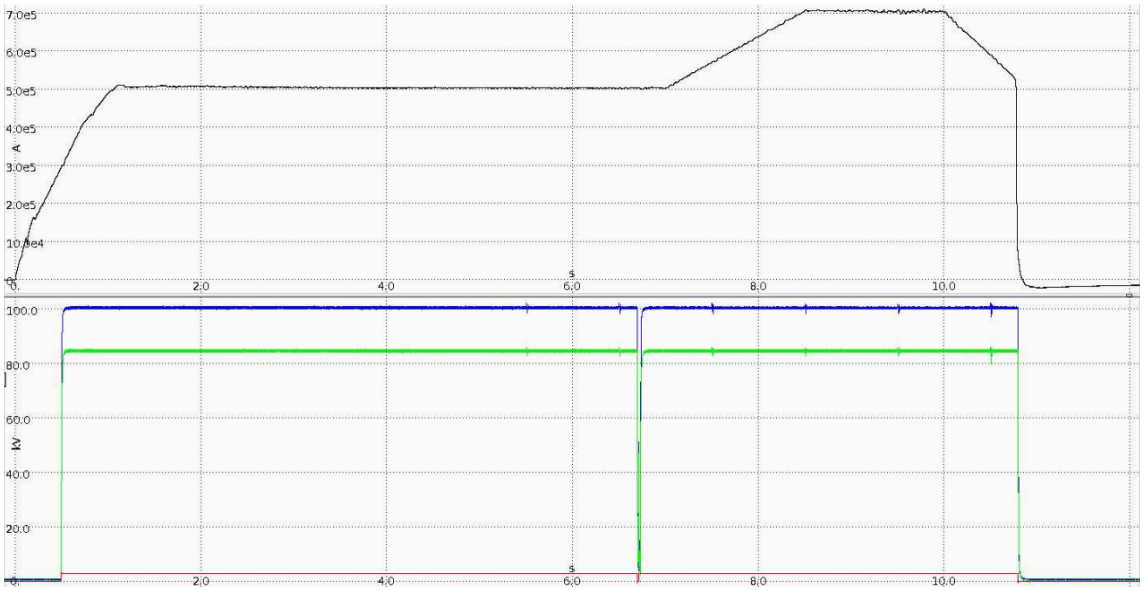

Figure 6. 40: Plasma current (up) and NBI voltage (down), with ION1 blue, ION2 green, ION3 red, for shot 14203.

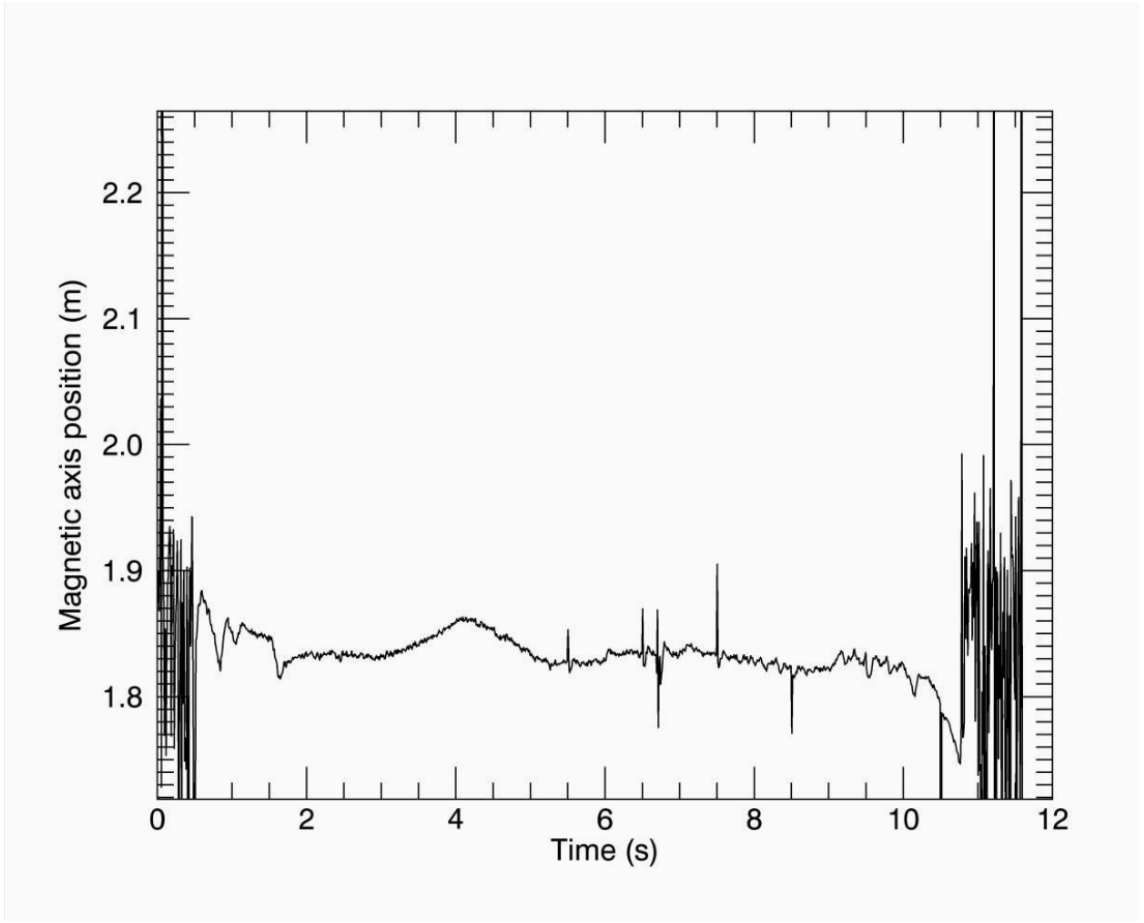

Figure 6. 41: Magnetic axis over time for shot 14203.

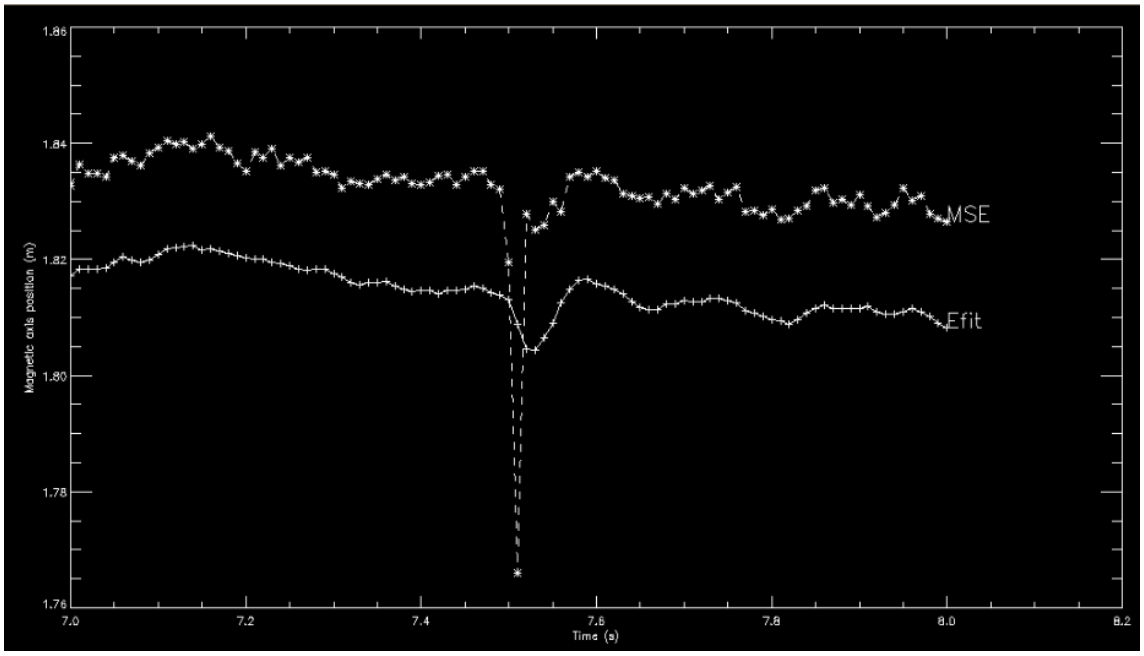

Figure 6. 42: Magnetic axis from MSE and EFIT, over t=7s – 8s for shot 14203.

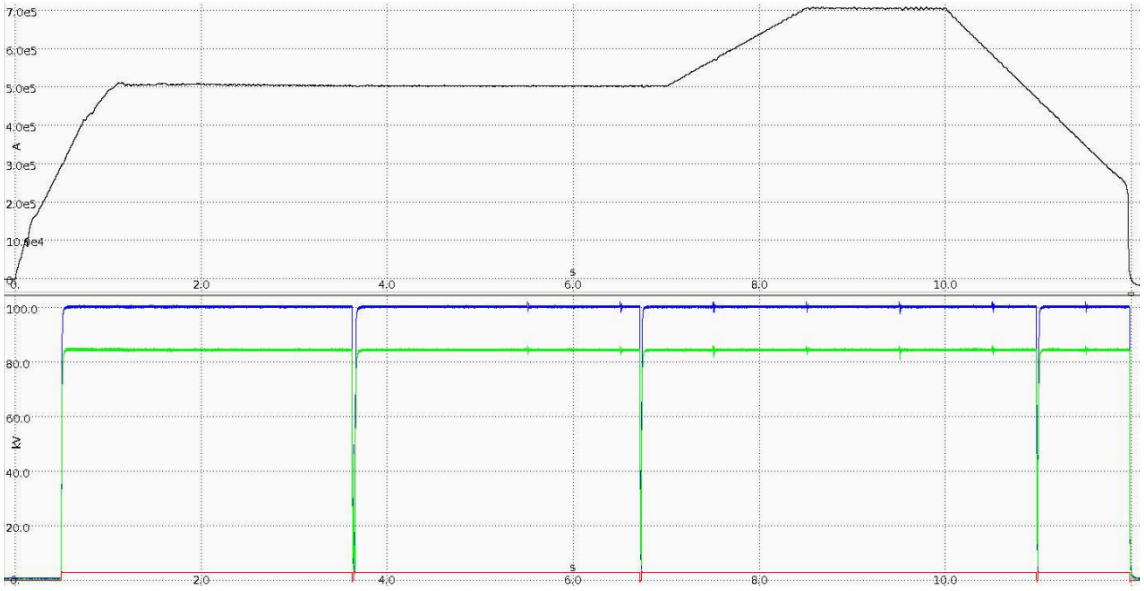

Figure 6. 43: Plasma current (up) and NBI voltage (down), with ION1 blue, ION2 green, ION3 red, for shot 14204.

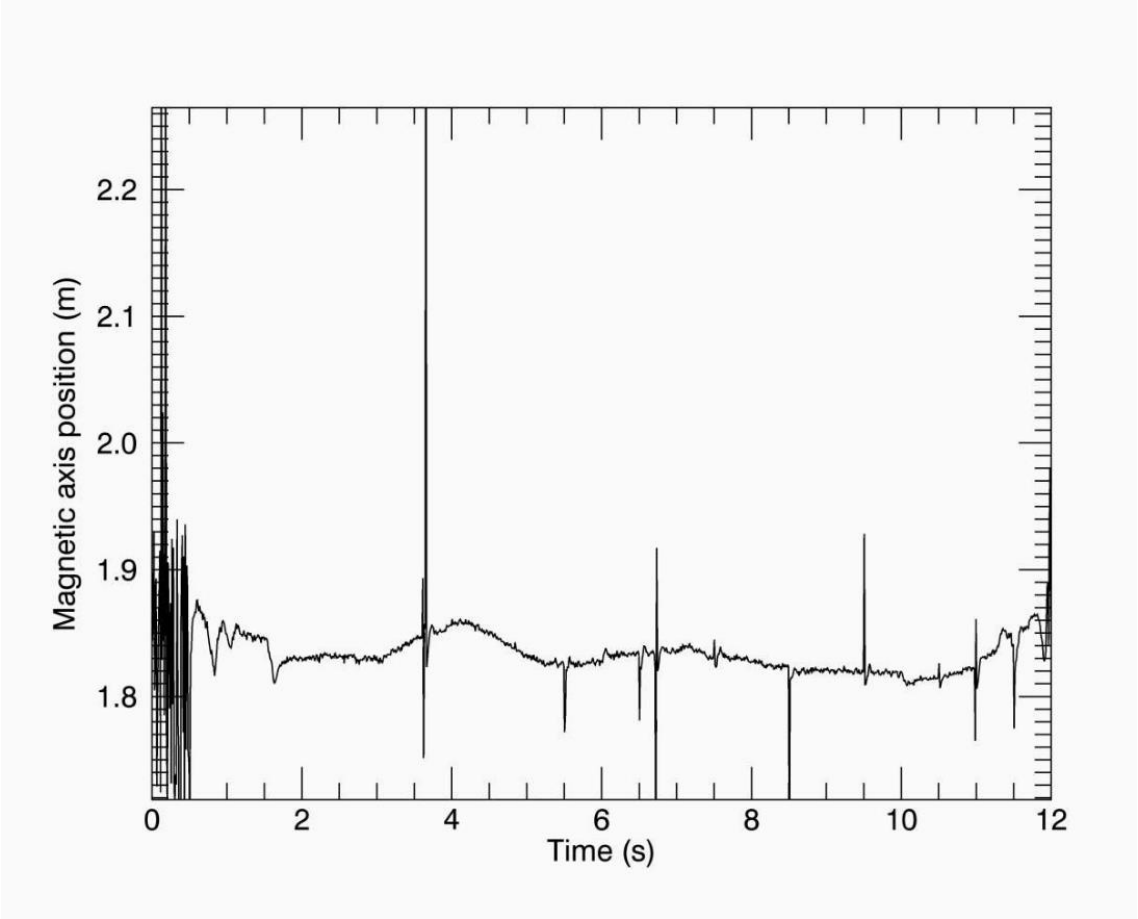

Figure 6. 44: Magnetic axis over time for shot 14204.

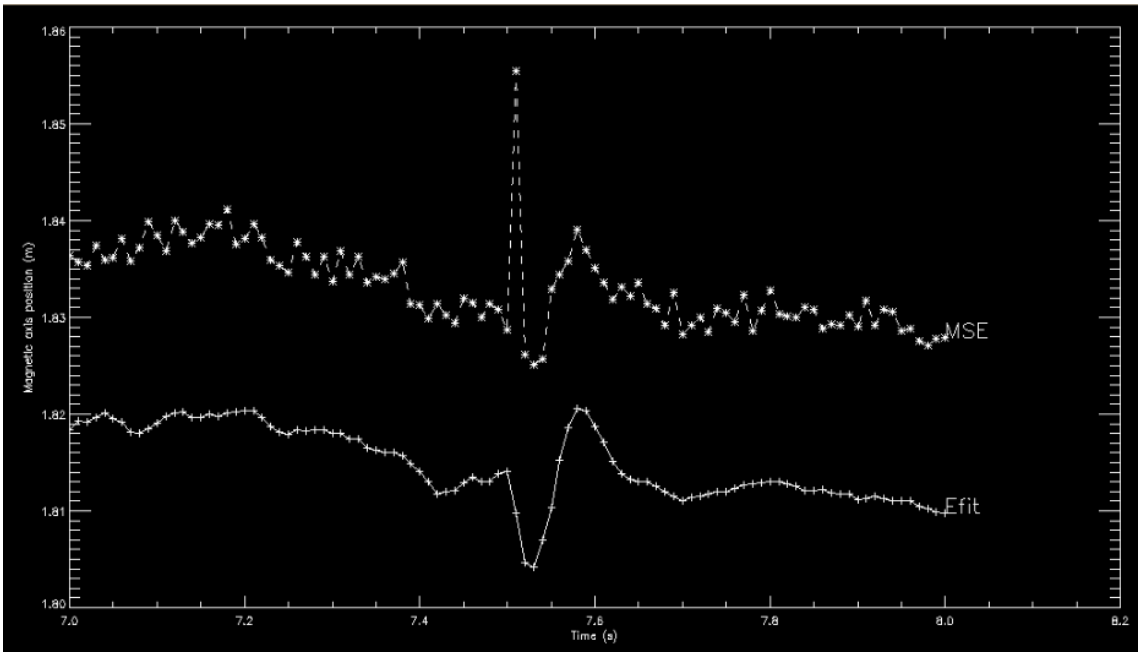

Figure 6. 45: Magnetic axis from MSE and EFIT, over t=7s – 8s for shot 14204.

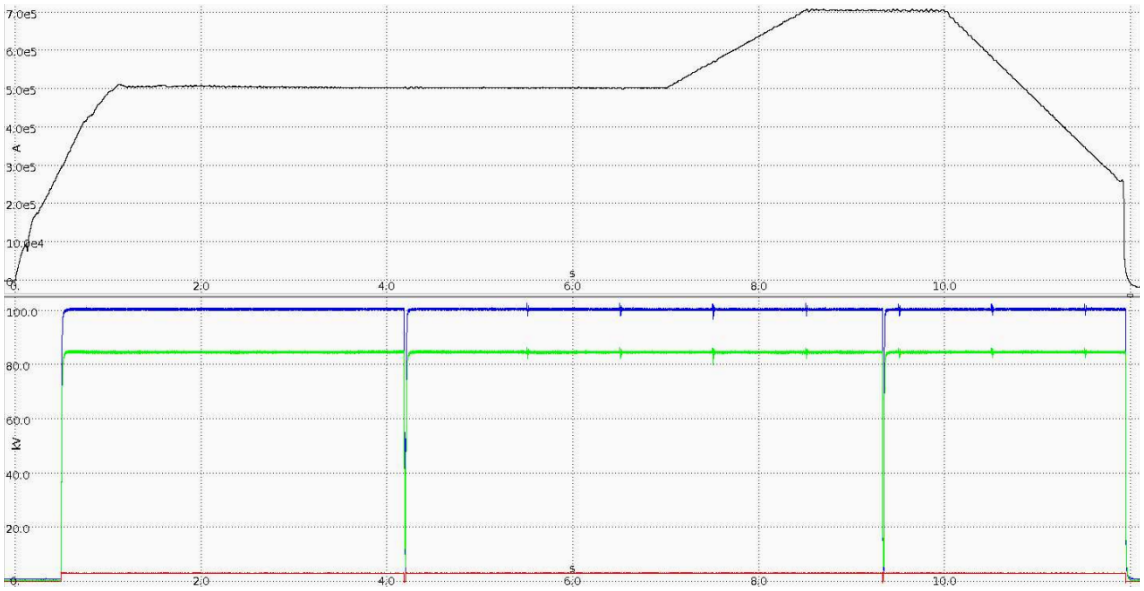

Figure 6. 46: Plasma current (up) and NBI voltage (down), with ION1 blue, ION2 green, ION3 red, for shot 14205.

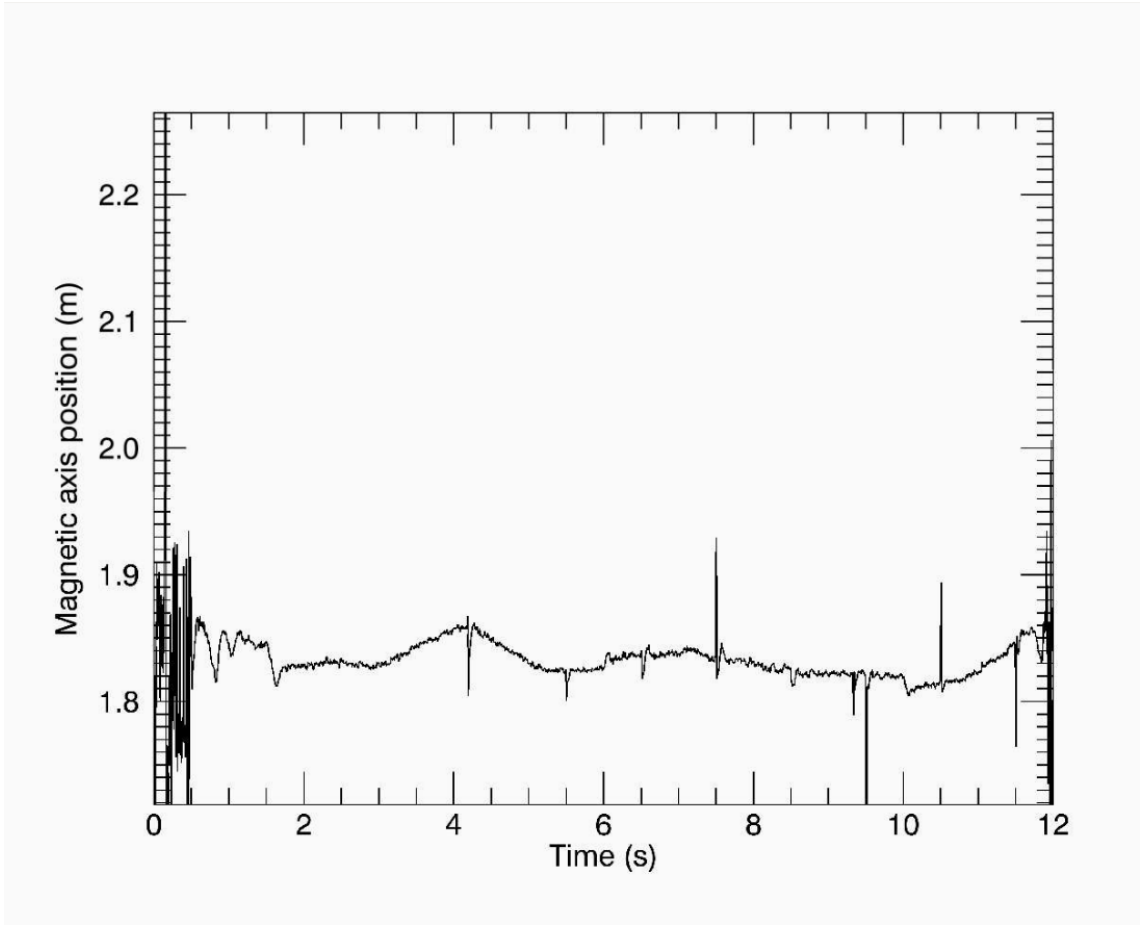

Figure 6. 47: Magnetic axis over time for shot 14205.

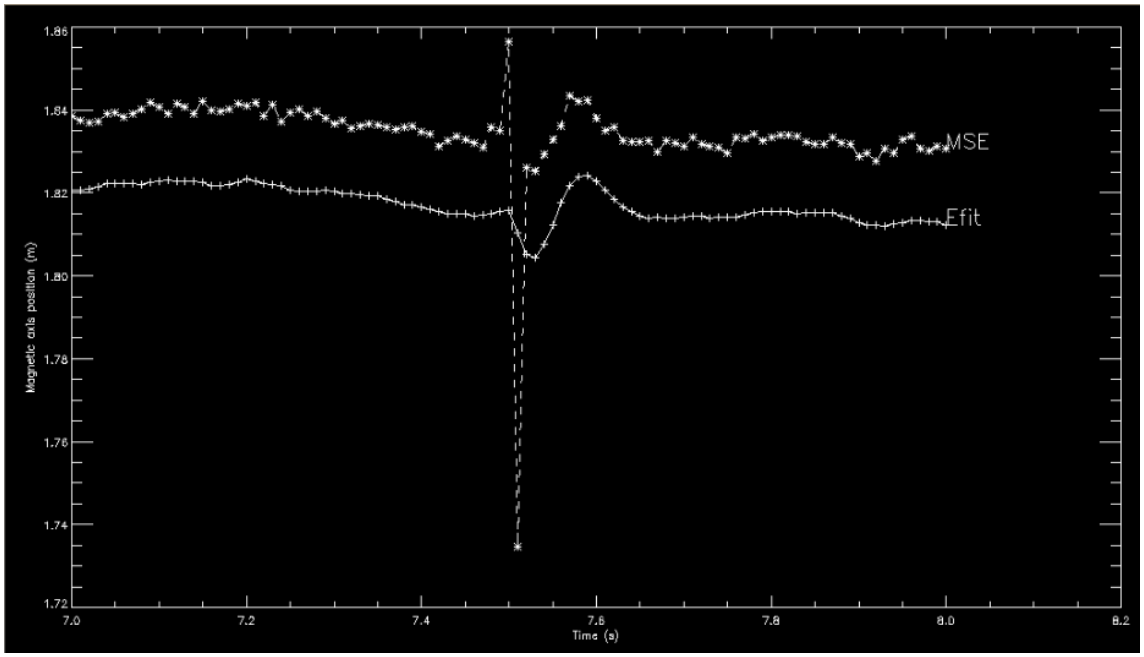

Figure 6. 48: Magnetic axis from MSE and EFIT, over t=7s – 8s for shot 14205.

6.2. Comments on the results

Group 1:

This group presents a plasma current that achieves a flat shape with a value of $I_p = 6 \cdot 10^5\ A$. The voltage values for ION1 and ION2 are 100kV and ~85kV respectively, so the condition of 15% reduction of ION2 voltage respect ION1 voltage is fulfilled.

It is observed a stable position of the magnetic axis over time with a slight difference in the value between the different shots of the group. The peaks are related to fluctuations on the ION voltage, for instance, for times 3.5s, 4.5s, 5.5s or 6.5s.

Regarding the EFIT verification, the results obtained from both are different. However, the behaviour tends to be similar.

Group 2:

The plasma current also has a flat shape with a value of $I_p = 5 \cdot 10^5\ A$ on that case. On the other hand, $V_{ION1} = 100\ kV$ and V_{ION2}~$85\ kV$ are the same as in group 1.

Respect the shots 13724 and 13725, the magnetic axis fluctuate over the time not only when the voltage or the current have a peak. The magnetic axis position seems to be out from the radius covered by the MSE channels.

On the other hand, for shots 13727 and 13728 the conclusions are the same as in the group 1.

Group 3:

In this case, even though the plasma current has a flat shape with value $I_p = 5 \cdot 10^5\ A$, it presents small fluctuation over all the time. The voltages $V_{ION1} = 80\ kV$ and V_{ION2}~$68\ kV$ only operate on a range time.

A clear plot of the magnetic axis is not obtained for any of the shots. Hence, no conclusions on the verification aspect are done.

Group 4:

This group plasma current is characterised by two flat regions $I_p^1 = 5 \cdot 10^5\ A$ and $I_p^2 = 7 \cdot 10^5\ A$. The voltages are $V_{ION1} = 100\ kV$ and V_{ION2}~$85\ kV$.

With regards to the magnetic axis is observed that the value is almost the same for all the shots with the exceptions of the different peaks caused by the peaks on the voltage, which are different for the different shots.

Respect the verification with EFIT, even though it exist a difference on the values, it is observed that magnetic axis from both MSE and EFIT tend to have the same behaviour, having a similar shape wave, only that MSE curve is ~0.02m above.

CONCLUSIONS

The main objective of this project is to obtain the magnetic axis evolution over time from the MSE system and to compare the result with EFIT modifying the existing codes. A derivation from this objective is to analyse different shots to observe how different parameters affect to the magnetic axis.

But to achieve this goal, before it is necessary to have a background. In the project the most relevant concepts are explained and summarised.

With regards to obtain the magnetic axis, the original code has to be modified. Hence, before to start to work with it, it is important to know the basic syntax of IDL and to be able to use the internal functions of the code.

It is also important to understand the different variables already existing on the code, how they are structured, which of them is useful for the updating, since some of them are used as an input. Furthermore, the already existing structure of the document is maintained on the updating in order to keep an structure and to be easily understood in some future.

Once the code is updated, it is used to analyse different shots with different plasma current and ion source voltages, in order to check if the magnetic axis position is affected by some of those. It is concluded that fluctuations on both the plasma current and the ion source voltage affect the magnetic axis.

By analysing different shots, among with the verification with EFIT, it is also tested the reliability, the strength and the flexibility of the MSE diagnosis.

APRECIATION

I would like to thank in first place Max Messmer for his guidance during the last 5 months. For trusting me, for teaching me different concepts essential for fusion and for have infinite patience when it was about writing the code.

At the same time, I want to acknowledge Dr Roger Jaspers from TU/e for giving me the opportunity to take place at this project and for supervising this thesis and Alfredo de Blas from UPC for his tutorship and advice.

I feel grateful to all the staff and members from TU/e for their support and effort to make me feel good.

As well I want to express my gratitude to FuseNet for making possible my stay.

And finally thanks to my mother Julia, my father Julio, my brothers Juli, Arturo and César and sister Celia, my grandfather Julián, my aunt-grandmother María Teresa, my sister in law Adriana, my mother's boyfriend Robert and my boyfriend Abu, for inspiring and supporting me, and for their help. Without them this project wouldn't have been possible.

BIBLIOGRAPHY

Bibliographical references

[1] IEA, International Energy Agency, *World Energy Outlook 2013*. London, 12 November 2014.

[2] IEA, International Energy Agency, *World Energy Outlook 2015 Presentation at the launch*. London, 10 November 2015.

[3] DIES, J. *Fusion Technology*. Barcelona – ETSEIB, 2014-2015.

[4] CALVIÑO, F. *Fundamentals of Nuclear Engineering and Radiological Protection; Atoms, Nuclei, Radioactivity, Interaction, Reactions; Nucleus*. Barcelona – ETSEIB, 2011-2012.

[5] MAX-PLANCK-INSTITUT FÜR PLASMAPHYSIK, *Tokamak*. Munich, 2003-2016. [http://www.ipp.mpg.de/14869/tokamak]

[6] FREUDENRICH, C. *How Nuclear Fusion Reactors Work*. How stuff works – Science. [http://science.howstuffworks.com/fusion-reactor4.htm]

[7] I.L. CALDAS, R.L. VIANA, M.S.T. ARAUJO, A. VANNUCCI, E.C. DA SILVA, K. ULLMANN, M.V.A.P. HELLER. *Control of Chaotic Magnetic Fields in Tokamaks*. Brazilian Journal of Physics, vol. 32, no. 4, Figure 11. São Paulo. Dec. 2002

[8] HÖLZL, M. *Diffusive Heat Transport across Magnetic Islands and Stochastics Layers in Tokamaks*. Figure 1.3. Technische Universität München, 29 January 2010.

[9] MAX-PLANCK-INSTITUT FÜR PLASMAPHYSIK. *ASDEX upgrade banishes instabilities*. Munich, 11 November 2004. [http://www.ipp.mpg.de/ippcms/eng/presse/archiv/08_04_pi]

[10] NFRI, National Fusion Research Institute, TU/e, Techische Universiteit Eindhoven. *A conventional Motional Stark Effect diagnostic for KSTAR*. Figure 1, Figure 2, Figure 10. January 2013 – March 2014.

Supplementary bibliography

[1] FUSENET. Fusion info; Basics. [http://www.fusenet.eu/node/30]

[2] FUSION FOR ENERGY. Understanding fusion. [http://fusionforenergy.europa.eu/understandingfusion/]

[3] CALVIÑO, F. *Fundamentals of Nuclear Engineering and Radiological Protection; Atoms, Nuclei, Radioactivity, Interaction, Reactions; Neutron Interaction I.* Barcelona, UPC, 2011-12

[4] HYPER PHYSICS. Nuclear Physics. Georgia State University. [http://hyperphysics.phy-astr.gsu.edu/hbase/hframe.html]

[5] DELABIE, E.G. *Neutral beam driven hydrogen spectroscopy in fusion plasmas*. PhD Thesis. Eindhoven, Technische Universiteit Eindhoven, 2011. 978-90-386-2480-8

[6] EUROPEAN FUSION NETWORK INFORMATION. About Fusion. [http://www.fusion-eur.org/]

[7] LOPES CARDOZO, N. *Fusion on the back of an envelope*. Eindhoven, Technische Universiteit Eindhoven, 2015-2016.

[8] F.M. LEVINTON, R.J. FONCK, G.M. GAMMEL, R. KAITA, H.W. KUGEL, E.T. POWELL, D.W. ROBERTS. *Magnetic Field Pitch-Angle Measurements in the PBX-M Tokamak Using the Motional Stark Effect*. The American Physical Society, vol. 63, no. 19. Princeton. 6 November 1989

[9] J. CHUNG, J. KO, J. HOWARD, C. MICHAEL, G. VON NESSI, A. THOMAS, M.F.M. DE BOCK. *Motional Stark Effect Diagnostics for KSTAR*. Journal of the Korean Physical Society, vol. 65, no. 8, pp 1257-1260. October 2014

[10] M. DE BOCK. *Summary of Stokes vectors, Müller matrices and harmonics for MAST MSE*. September 11, 2009

[11] HARRIS GEOSPATIAL SOLUTIONS, *IDL reference.* [http://www.harrisgeospatial.com/docs/routines-1.html]